

AD-A194 593

COUPLING BETWEEN RADIATION AND GAS DYNAMICS(U)

1/1

PENNSYLVANIA STATE UNIV UNIVERSITY PARK DEPT OF

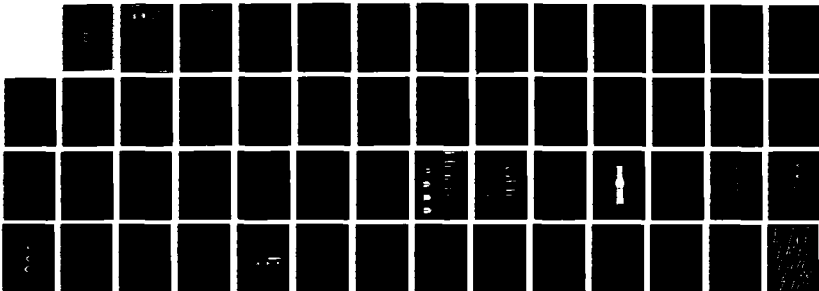
MECHANICAL ENGINEERING C L MERKLE ET AL 01 MAR 88

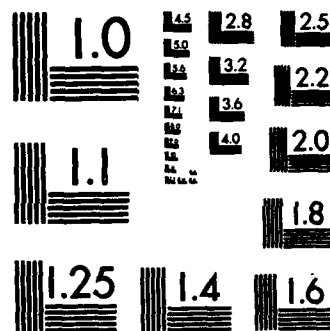
UNCLASSIFIED

AFOSR-TR-88-0448 AFOSR-84-0048

F/G 28/4

NL





UNCLASSIFIED

SECURITY CLASSIFICATION

REPORT DOCUMENTATION PAGE

2

AD-A194 593

IC

1b. RESTRICTIVE MARKINGS

DTIC FILE COPY

2b. DECLASSIFICATION/DOWNGRADING SCHEDULE

NA

MAY 03 1988

3. DISTRIBUTION/AVAILABILITY OF REPORT

Approved for Public Release
Distribution is Unlimited

4. PERFORMING ORGANIZATION REPORT NUMBER(S)

None

5. MONITORING ORGANIZATION REPORT NUMBER(S)

AFOSR-TR- 88-0448

6a. NAME OF PERFORMING ORGANIZATION

Pennsylvania State University

6b. OFFICE SYMBOL
(If applicable)

7a. NAME OF MONITORING ORGANIZATION

AFOSR

6c. ADDRESS (City, State and ZIP Code)

Mechanical Engineering Department
University Park, PA 16802

7b. ADDRESS (City, State and ZIP Code)

same &c.

8a. NAME OF FUNDING/SPONSORING
ORGANIZATION Air Force

Office of Scientific Research

8b. OFFICE SYMBOL
(If applicable)

NA

9. PROCUREMENT INSTRUMENT IDENTIFICATION NUMBER

AFOSR-84-0048

8c. ADDRESS (City, State and ZIP Code)

Bolling AFB, Washington, D.C. 20332

Bldg 410

10. SOURCE OF FUNDING NOS.

PROGRAM
ELEMENT NO.PROJECT
NO.TASK
NO.WORK UNIT
NO.

61102F

2308

A1

11. TITLE (Include Security Classification)

Coupling Between
Radiation and Gas Dynamics

12. PERSONAL AUTHOR(S)

Charles L. Merkle and Michael M. Micci

13a. TYPE OF REPORT

Annual

13b. TIME COVERED

FROM 01 Feb 87 TO 01 Feb 88

14. DATE OF REPORT (Yr., Mo., Day)

1988, March 1

15. PAGE COUNT

49

16. SUPPLEMENTARY NOTATION

17. COSATI CODES

FIELD

GROUP

SUB. GR.

18. SUBJECT TERMS (Continue on reverse if necessary and identify by block number)

Laser/Gasdynamics Interaction,
Microwave Heating of GasesBeamed Energy,
Advanced Propulsion

19. ABSTRACT (Continue on reverse if necessary and identify by block number)

Direct heat addition of flowing gases by radiation absorption is considered. In the visible wavelength regime, the interaction between concentrated solar energy and a flowing gas is being modeled numerically. Additional analyses of laser-gasdynamics interactions are also being considered. Implicit time-iterative procedures originally developed for transonic flows are being adapted to the low Mach number, low Reynolds number regimes of interest. Two-dimensional solutions show that absorption plasmas can exist over a wide range of flow speeds and that buoyancy is a dominant factor in the forced convection flowfields. In the microwave regime, an experimental investigation of various absorption modes is underway. An overview of the microwave resonant cavity experiment and initial experimental results with nitrogen is presented. Numerical predictions of the planar and propagating plasma mode of microwave absorption in hydrogen, helium and nitrogen are also discussed.

20. DISTRIBUTION/AVAILABILITY OF ABSTRACT

UNCLASSIFIED/UNLIMITED ☒ SAME AS RPT. ☒ DTIC USERS ☐

21. ABSTRACT SECURITY CLASSIFICATION

Unclassified

22a. NAME OF RESPONSIBLE INDIVIDUAL

Dr. Mithat Birkan

22b. TELEPHONE NUMBER
(Include Area Code)

(202) 767-4938

22c. OFFICE SYMBOL

AFOSR/NA

APOSR-TX. 88-0448

Annual Report

on

**COUPLING BETWEEN RADIATION
AND GAS DYNAMICS**

Submitted to:

Dr. Mithat Birkan
Air Force Office of Scientific Research
Directorate of Aerospace Sciences
Bolling Air Force Base, D.C. 20332

by

Dr. Charles L. Merkle
Mechanical Engineering Department
The Pennsylvania State University
University Park, PA 16802
(814) 863-1501

and

Dr. Michael M. Micci
Aerospace Engineering Department
The Pennsylvania State University
University Park, PA 16802
(814) 863-0043

Accession For	
NTIS CRA&I	<input checked="checked" type="checkbox"/>
DTIC TAB	<input type="checkbox"/>
Unannounced	<input type="checkbox"/>
Justification	
By	
Distribution /	
Availability Codes	
Dist	Avail and/or Special
A-1	

February 1988



88 5_02 160

TABLE OF CONTENTS

	<u>Page</u>
ABSTRACT.....	1
STATEMENT OF WORK.....	2
STATUS OF RESEARCH EFFORT.....	3
FIGURES.....	6
REFERENCES.....	12
CUMULATIVE CHRONOLOGICAL LIST OF WRITTEN PUBLICATIONS IN TECHNICAL JOURNALS.....	13
PROFESSIONAL PERSONNEL ASSOCIATED WITH RESEARCH EFFORT.....	14
INTERACTIONS.....	15
 I. STATUS OF RESEARCH EFFORT.....	16
FIGURES.....	25
II. CUMULATIVE CHRONOLOGICAL LIST OF WRITTEN PUBLICATIONS.....	44
III. PROFESSIONAL PERSONNEL ASSOCIATED WITH RESEARCH EFFORT.....	46
IV. INTERACTIONS/SPOKEN PRESENTATIONS.....	47
V. INTERACTIONS/ADVISORY FUNCTIONS.....	49
VI. NEW DISCOVERIES.....	49

ABSTRACT

Direct heat addition of flowing gases by radiation absorption is considered. In the visible wavelength regime, the interaction between concentrated solar energy and a flowing gas is being modeled numerically. Additional analyses of laser-gasdynamic interactions are also being considered. Implicit time-iterative procedures originally developed for transonic flows are being adapted to the low Mach number, low Reynolds number regimes of interest. Two-dimensional solutions show that absorption plasmas can exist over a wide range of flow speeds and that buoyancy is a dominant factor in the forced convection flowfields. In the microwave regime, an experimental investigation of various absorption modes is underway. An overview of the microwave resonant cavity experiment and initial experimental results with nitrogen is presented. Numerical predictions of the planar and propagating plasma mode of microwave absorption in hydrogen, helium and nitrogen are also discussed.

Statement of Work

1. Determine experimentally the conditions under which plasmas can be initiated and sustained in the three energy addition modes (TM_{01} , TE_{01} , and planar). Initial testing will be with nitrogen and helium. Nitrogen will be used to simulate the molecular nature of hydrogen while helium will simulate atomic hydrogen. Final testing will be with hydrogen. Parameters to be examined include gas composition, pressures and flow rates and microwave power. Quantify system heat losses.
2. Measure spectroscopically electron and ion temperatures and densities in microwave generated plasmas in the three energy addition modes. Due to high gas pressures, local thermodynamic equilibrium (LTE) will be initially assumed although nonequilibrium effects will be examined. The principal measurement will be ion temperature as this translates to thrust. The effects of various hot and cold gas mixing schemes on final temperature will be studied.

Status of Research Effort

Free-floating spherical plasmas have been generated in stationary nitrogen gas contained inside a spherical quartz vessel located within a cylindrical resonant cavity operated in the TM_{012} mode. The plasmas are approximately two inches in diameter and are centered within the five inch ID quartz sphere. Power coupled to the plasma was measured as a function of nitrogen pressure and microwave power input to the cavity only for those combinations of pressure and power which resulted in the plasma being stabilized in the center of the quartz sphere away from adjacent walls. Figure 1 plots the coupling efficiency as a function of absolute pressure for several input power levels. The coupling efficiency is defined to be the percentage of input microwave power actually absorbed in the gas. It can be seen that the coupling efficiency rises with increased pressure but decreases with increased power. Figure 2 plots the total microwave power absorbed by the gas and shows that the total power absorbed initially increases with both increased input power and gas pressure but levels off above input powers of 350 W and gas pressures of 15 kPa. Figure 3 plots the maximum coupling efficiency obtained from Figure 1 as a function of input power and shows the coupling efficiency dropping from 80% to 30% as the input power is raised from 100 to 500 W.

A numerical model of the one-dimensional planar propagating microwave plasma in hydrogen, helium and nitrogen gas has been successfully formulated.¹ This model numerically integrates the system of governing equations consisting of the one-dimensional steady energy equation

$$\rho u C_p \frac{dT}{dx} = \frac{d}{dx} \lambda \frac{dT}{dx} + \frac{\sigma}{2} |E|^2 \quad (1)$$

where ρ is the gas density, u is the gas velocity, C_p is the specific heat, T is the gas temperature, λ is the thermal conductivity, σ is the electrical conductivity and E is the electric field vector; and Maxwell's equation describing the propagation of the microwave energy

$$\frac{d^2 E}{dx^2} = \sigma \mu \frac{\partial E}{\partial t} + \epsilon \mu \frac{\partial^2 E}{\partial t^2} \quad (2)$$

where ϵ is the permittivity and μ is the permeability. The specific heat, thermal conductivity and electrical conductivity are functions of temperature. The electromagnetic energy is absorbed by the plasma as the temperature rises with some microwave energy being reflected or transmitted. Due to thermal conduction to the cold gas ahead of it, the plasma propagates toward the microwave energy source at a velocity determined by the energy balance between the absorbed microwave power and the heated gas which is convected away downstream.

The two governing equations were numerically integrated using a fifth/sixth order variable step Runge-Kutta scheme. An iterative method was used to determine the propagation velocity eigenvalue, ρu , similar to the method used by Kemp and Root² to solve for the propagation velocity of the laser heated plasma. The propagation velocity, maximum temperature and percent power absorbed were calculated as functions of the input microwave power. Figure 4 plots the propagation velocity as a function of input power and shows the propagation velocity rising with increased microwave power. The decreased velocity for the higher gas pressure is primarily due to the increased gas density since ρu is the propagation eigenvalue and is almost equal for the two gas pressures. Figure 5 plots the maximum gas

temperature as a function of input power while Figure 6 plots both the percent power absorbed and the percent power reflected by the propagating plasma as a function of input power. The maximum gas temperature is constant for hydrogen and nitrogen because significant dissociation is occurring in this temperature range and is absorbing the additional absorbed power. The maximum gas temperature for helium, which is not dissociating, is seen to rise with increasing input power. It was found that all of the input power was either reflected or absorbed with no power being transmitted through the plasma and that the percent power absorbed for hydrogen decreases with increased input power while the percent power absorbed for helium and nitrogen remained fairly constant as a function of input microwave power. The results of the numerical model will be compared to experimentally measured values as they become available.

Coupling Efficiency Versus Absolute Pressure for Various Input Powers

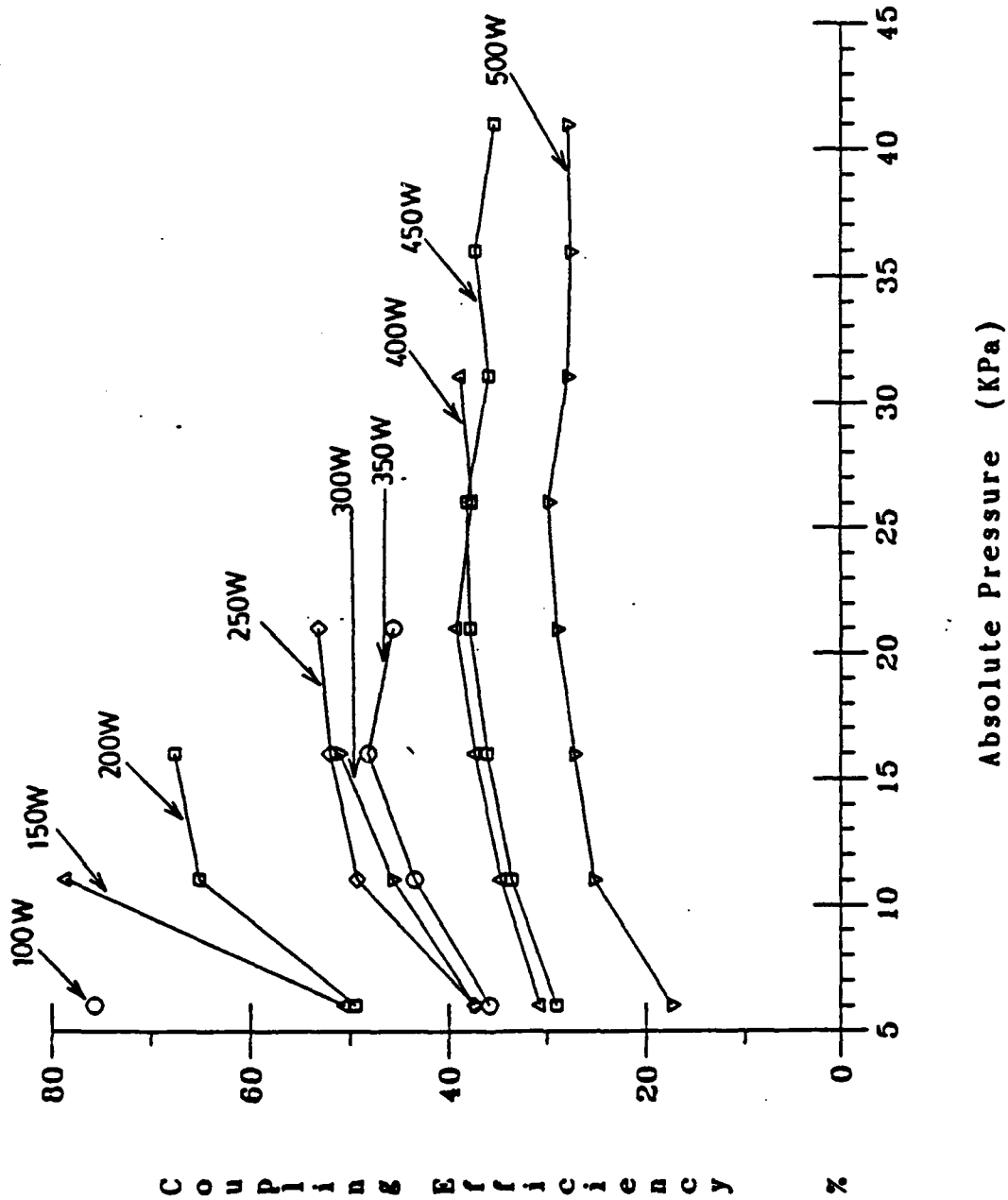


Fig. 1 Coupling efficiency of a free-floating spherical plasma in stationary nitrogen gas as a function of absolute pressure for several input microwave power levels.

Power Coupled to the Plasma Versus Absolute Pressure

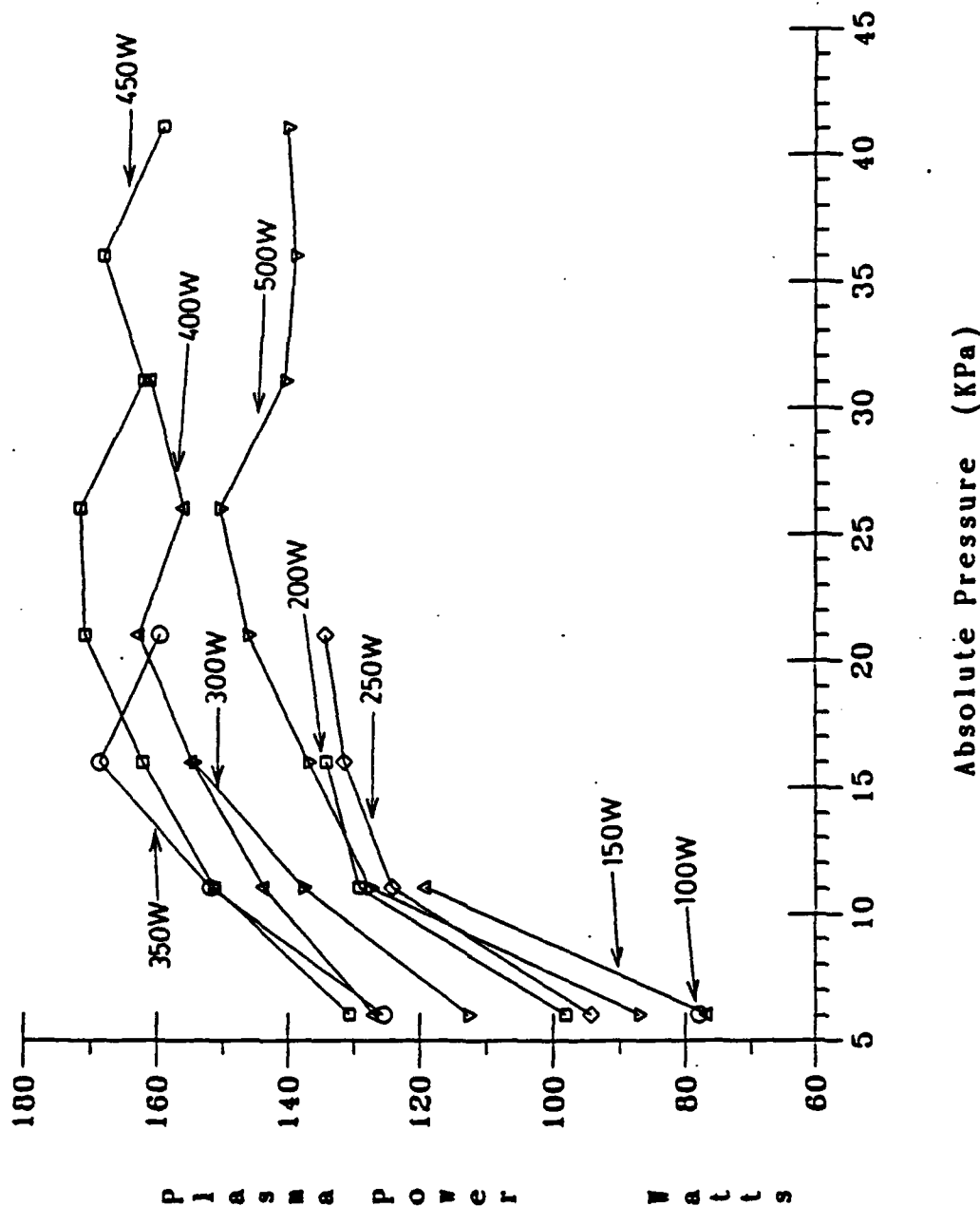
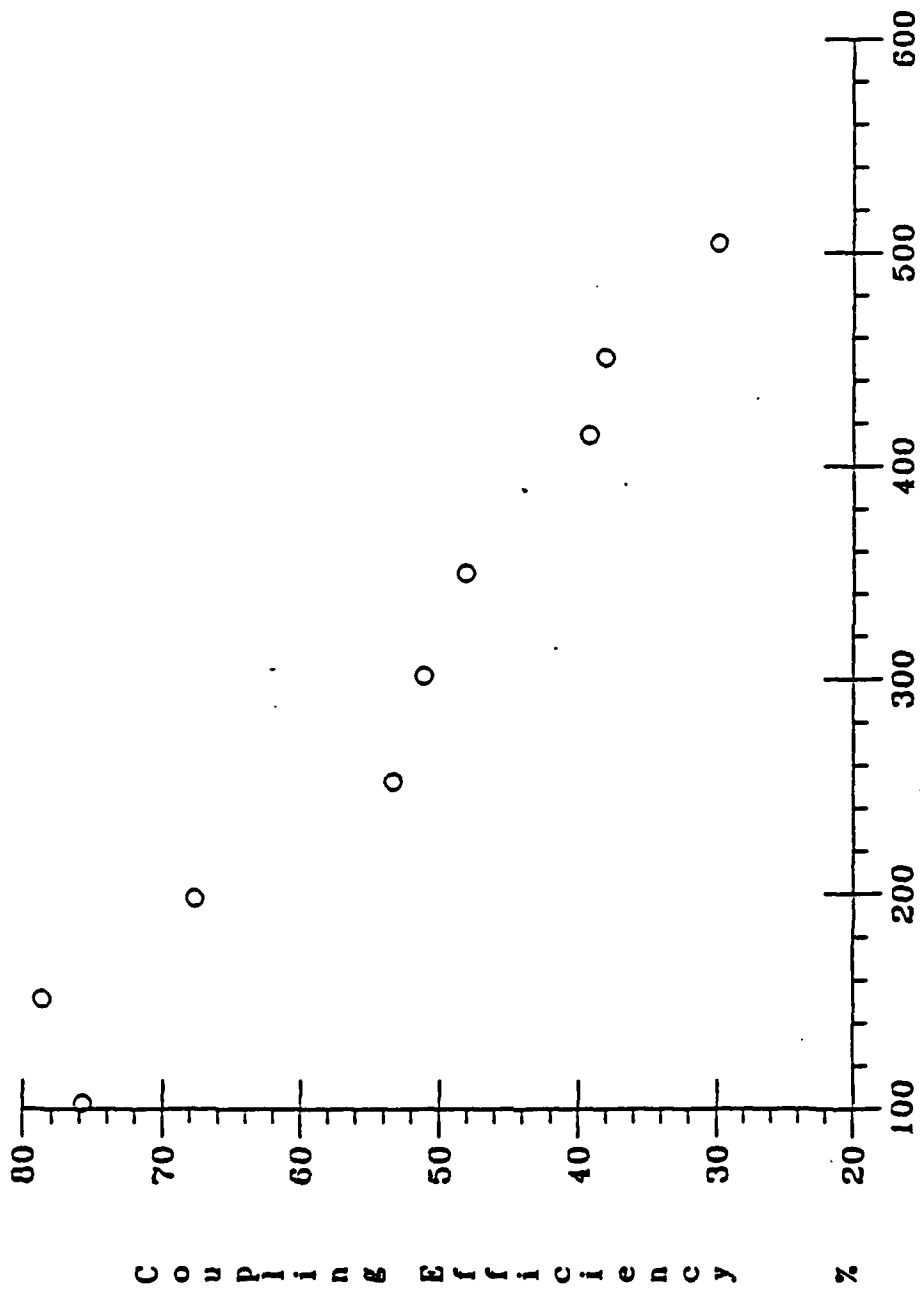


Fig. 2 Total microwave power coupled to a free-floating spherical plasma in stationary nitrogen gas as a function of absolute pressure for several input power levels.

Maximum Coupling Efficiency Versus Input Power



Input Power (Watts)

Fig. 3 Maximum coupling efficiency to a free-floating spherical plasma in stationary nitrogen gas as a function of input microwave power.

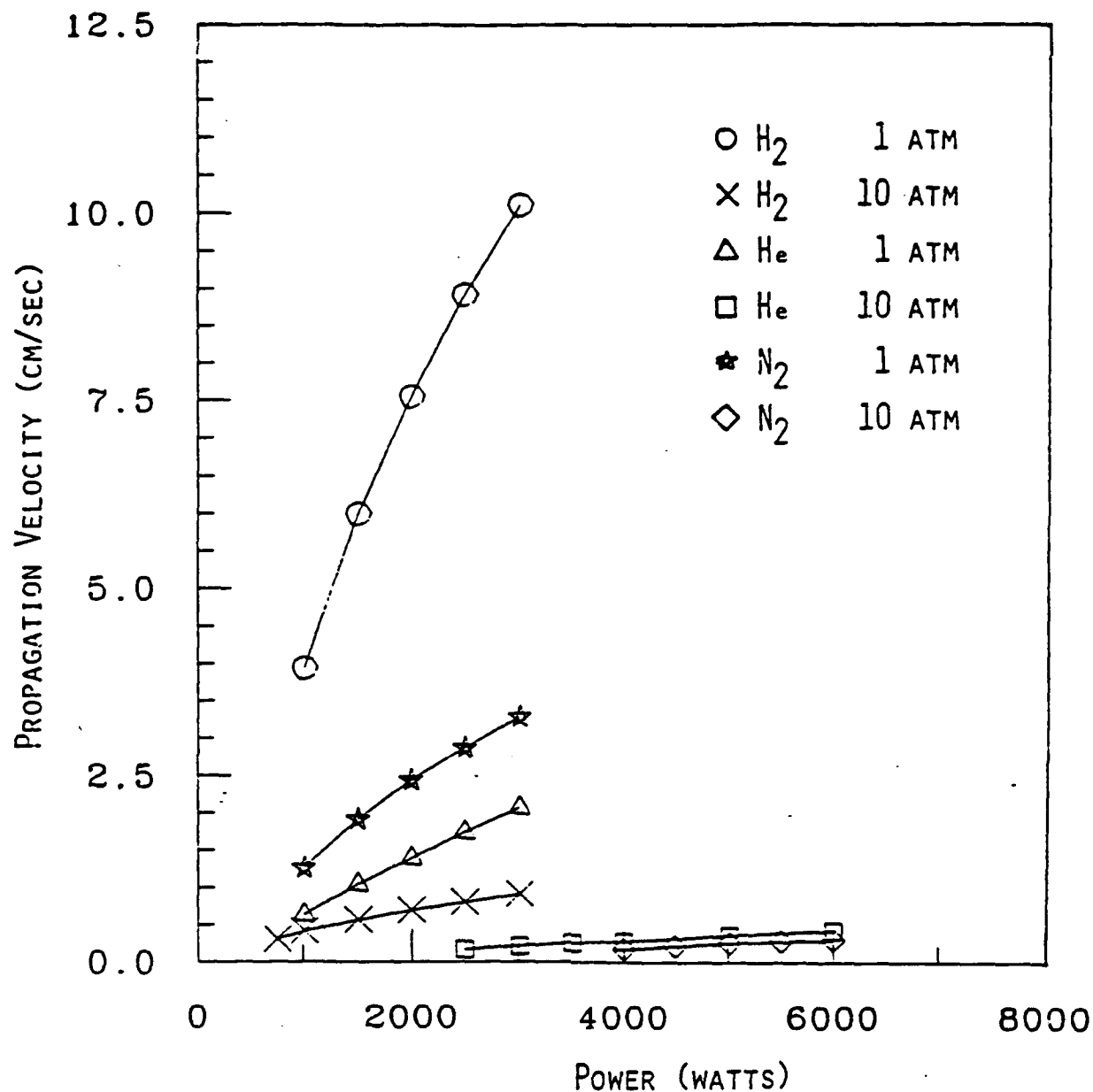


FIG. 4 MICROWAVE HEATED PLANAR PLASMA PROPAGATION VELOCITY VERSUS INPUT POWER FOR HYDROGEN, HELIUM AND NITROGEN SHOWING INCREASED PLASMA WAVE VELOCITY WITH INCREASED POWER.

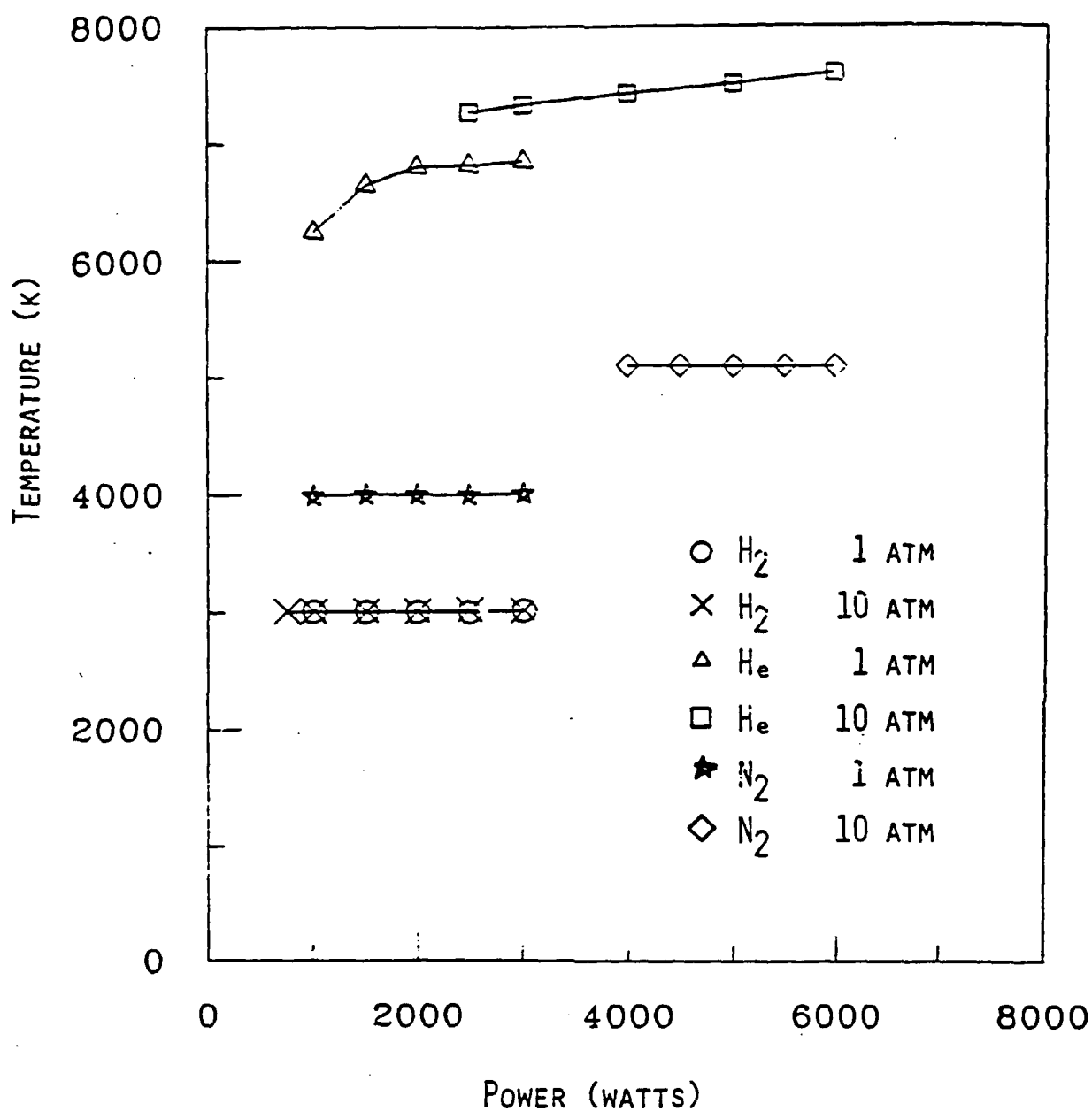


FIG. 5 MAXIMUM MICROWAVE HEATED PLASMA TEMPERATURE VERSUS INPUT POWER FOR HYDROGEN, HELIUM AND NITROGEN SHOWING TEMPERATURE DIFFERENCES BETWEEN GASES BUT SMALL INCREASE IN TEMPERATURE WITH INCREASED POWER.

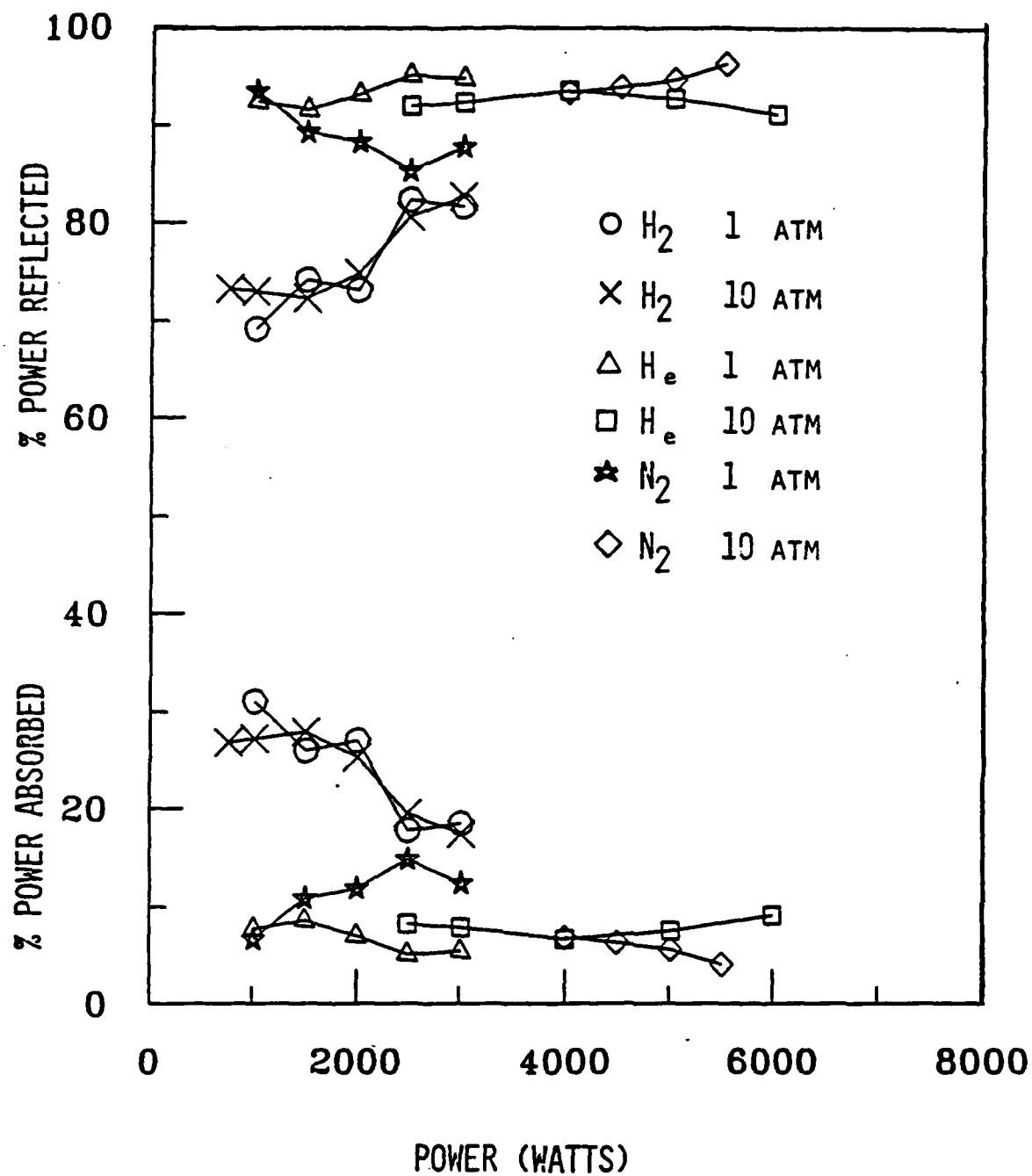


FIG. 6 PERCENT INCIDENT POWER ABSORBED AND REFLECTED AS A FUNCTION OF INPUT POWER FOR HYDROGEN, HELIUM AND NITROGEN.

References

1. Durbin, M. R. and Micci, M. M., "Analysis of Propagating Microwave Heated Plasmas in Hydrogen, Helium and Nitrogen," AIAA Paper 87-1013, May, 1987.
2. Kemp, N. H. and Root, R. G., "Analytical Study of Laser-Supported Combustion Waves in Hydrogen," Journal of Energy, Vol. 3, No. 1, Jan.-Feb., 1979, pp. 40-49.

Cumulative Chronological List of Written Publications in Technical Journals

1. Knecht, J. P. and Micci, M. M., "Analysis of a Microwave-Heated Planar Propagating Hydrogen Plasma," scheduled for publication in AIAA Journal.
2. Durbin, M. R. and Micci, M. M., "Analysis of Propagating Microwave Heated Plasmas in Hydrogen, Helium and Nitrogen," AIAA Paper 87-1013. Submitted for publication in Journal of Propulsion and Power.

Professional Personnel Associated with Research Effort

Professional Staff

Michael M. Micci, Assistant Professor, Aerospace Engineering

Graduate Students

James P. Knecht, Graduate Assistant, January 1985-May 1986. M. S. Thesis title, "Numerical Analysis of a Microwave-Heated Planar Propagating Hydrogen Plasma." Present position: MIT Lincoln Labs, Lexington, MA.

William Maul, Graduate Assistant, June 1985-December 1987. M. S. Thesis title, "The Characteristics of a Stationary Free-Floating Nitrogen Discharge Generated in a Microwave Resonant Cavity."

Juergen Mueller, Graduate Assistant, August 1987-present. Anticipated M.S. Thesis title, "Analytical and Experimental Study of Propagating Microwave-Heated Plasmas."

Philip Balaam, Graduate Assistant, August 1987-present. Anticipated Ph.D. Thesis title, "Investigation of Resonant Cavity Microwave-Heated Plasmas."

Interactions

(1) Spoken papers

Coupling Between Gas Dynamics and Microwave Energy Absorption.
Presented at the AFOSR/AFRPL Rocket Propulsion Research Meeting, March 21, 1985, Lancaster, CA.

Prospects for Microwave Heated Propulsion. Presented at Aerojet Tech Systems, Sacramento, CA, Oct. 8, 1985.

Prospects for Microwave Heated Propulsion. Presented to Project Forecast II, November 19, 1985, Arlington, VA.

Coupling Between Gas Dynamics and Microwave Energy Absorption.
Presented at the AFOSR/AFRPL Rocket Propulsion Research Meeting, September 11, 1986, Lancaster, CA.

Microwave Electrothermal Propulsion. Presented at the Air Force Office of Scientific Research, Bolling AFB, DC, September 18, 1986.

Analysis of Propagating Microwave Heated Plasmas in Hydrogen, Helium and Nitrogen. Presented at the 19th AIAA/DGLR/JSASS International Electric Propulsion Conference, May 12, 1987, Colorado Springs, CO.

Coupling Between Gas Dynamics and Microwave Energy Absorption.
Presented at the AFOSR/ONR Combustion and Rocket Propulsion Contractors Meeting, June 26, 1987, State College, PA.

Microwave Electrothermal Propulsion. Presented at Purdue University, July 13, 1987, W. Lafayette, IN.

Microwave Electrothermal Propulsion. Presented at The Ohio State University, September 8, 1987, Columbus, OH.

Annual Report

on

ANALYTICAL MODELING OF STRONG RADIATION
GAS-DYNAMIC INTERACTION

Submitted to:

Dr. Mithat Birkan
Air Force Office of Scientific Research
Directorate of Aerospace Sciences
Bolling Air Force Base, D.C. 20332

by

Dr. Charles L. Merkle
Mechanical Engineering Department
The Pennsylvania State University
University Park, PA 16802
(814) 863-1501

February 1988

I. STATUS OF RESEARCH EFFORT

A. Computational Algorithm

The advanced computational algorithms that have been developed for transonic, external aerodynamics in the past decade are being adapted for low speed flows with strong heat addition. The specific area of focus has been on the computation of the interaction between concentrated solar radiation and flowing gases, but the techniques are equally applicable to laser-gasdynamic interactions and microwave absorption, as well as to the more traditional combustion problems that occur in propulsion environments. The family of techniques being addressed is time dependent procedures. These are attractive because they apply to either viscous or inviscid flows and provide high accuracy and efficiency. In addition, time dependent procedures are applicable to either steady or unsteady flows, making them candidates for studying both the steady flow characteristics of propulsion environments as well as the linear and nonlinear stability characteristics of these flowfields.

The extension of time dependent algorithms from external transonic flows to internal propulsion environments required advances in several directions. The methods had to be modified to handle very low Mach number flows (which are nonetheless compressible because of the energy deposition) in addition to the transonic flows for which they were developed. In addition, they had to be extended from high Reynolds number applications to low Reynolds number conditions because some of the energy deposition processes described above take place at low Reynolds numbers. The modifications which enabled these low Mach number and low Reynolds number extensions are discussed below.

The equations of motion for a flowing gas with heat addition (by absorption of radiation, I²R heating, or combustion) can be expressed in vector form as,

$$\frac{\partial Q}{\partial t} + \frac{\partial E}{\partial x} + \frac{\partial F}{\partial y} = H + \frac{\partial E_v}{\partial x} + \frac{\partial F_v}{\partial y} \quad (1)$$

Here, Q , E , F , H , E_v and F_v are vectors. The primary dependent variables are contained in Q while the remaining five vectors are nonlinear functions of Q . These vectors are defined as,

$$Q = \begin{bmatrix} \rho \\ \rho u \\ \rho v \\ e \end{bmatrix} \quad E = \begin{bmatrix} \rho u \\ \rho u^2 + p \\ \rho uv \\ (e+p)u \end{bmatrix} \quad F = \begin{bmatrix} \rho v \\ \rho uv \\ \rho v^2 + p \\ (e+p)v \end{bmatrix} \quad H = \begin{bmatrix} 0 \\ pg \\ 0 \\ q \end{bmatrix}$$

and,

$$E_v = R_{xx} \frac{\partial Q_v}{\partial x} + R_{xy} \frac{\partial Q_v}{\partial y}$$

$$F_v = R_{yx} \frac{\partial Q_v}{\partial x} + R_{yy} \frac{\partial Q_v}{\partial y}$$

where $Q_v = (\rho, u, v, T)^T$, and R_{xx} , R_{xy} , R_{yx} , and R_{yy} are matrices containing only the viscosity and the thermal conductivity. For computational purposes, the equations are transformed to generalized nonorthogonal coordinates. Convergence to a steady state corresponds to following Eqn. 1 through a transient from some arbitrary initial condition to a final steady condition. We begin by discussing the inviscid terms on the left-hand side and then add the viscous terms on the right-hand side.

An example of the manner in which typical time dependent methods are slowed down as the flow Mach number is reduced is given in Fig. 1. The

reason for the decreased efficiency is because the eigenvalues of the system become increasingly stiff as Mach number is reduced. We have developed two methods for circumventing this problem. In the first, the time derivatives are multiplied by some matrix Γ which is chosen in such a way that the eigenvalues remain well conditioned at low Mach numbers. This matrix preconditioning procedure corresponds to modifying the physical time derivatives to control the acoustic speeds and provide faster convergence. The convergence of an inviscid problem with this preconditioning is shown in Fig. 2 for Mach numbers down to 10^{-5} . As can be seen from the figure, preconditioning allows us to maintain rapid convergence to low Mach numbers but eventually round-off errors are encountered in the pressure computations. These round-off errors prevent the use of the procedure at Mach numbers below about 10^{-4} . A summary of some initial preconditioning results is given in Ref. 9.

The second method for accomplishing low Mach number computations has been to use a perturbation expansion of the equations of motion to obtain a low Mach number system. In this low Mach number system, artificial acoustic modes are introduced to provide a well-conditioned eigenvalue system at any Mach number. This system also includes a rescaling of the pressure and all inviscid applications have shown it to be very effective. We have again obtained Mach number independent convergence to Mach numbers as low as 10^{-6} which exceeds the low speed range of the laser propulsion problems of interest and the pressure scaling eliminates the premature round-off errors noted with preconditioning. The low Mach number expansion procedure is described in Refs. 9, 10 and 12. Representative convergence rates for the low Mach number scheme are given in Fig. 3.

The addition of viscous terms to this low Mach number algorithm results in slightly enhanced convergence rates at higher Reynolds number ($Re = 1000$) as compared with inviscid conditions ($Re = \infty$) but at lower Reynolds numbers the convergence rates begin to decrease again as shown on Fig. 4. Unfortunately, $Re = 10$ is representative of laser absorption conditions. These reduced convergence rates at low Reynolds numbers can be avoided by proper rescaling of the time step (as discussed in detail in Ref. 12). Representative results for an optimum time step are given in Fig. 5. The convergence rates given here are for Mach number and Reynolds number conditions representative of those in solar or laser absorption regimes.

An example of flowfields calculated with this algorithm for Reynolds numbers from infinity (inviscid) to $Re = 0.05$ are shown on Fig. 6 for flow in a duct with a specified rate of volumetric heat addition. These various flow regimes include all conditions expected in beamed energy propulsion systems from the energy absorption regime through the throat. Similar calculations for energy addition through wall heating are given in Fig. 7. The overall domain of convergence in a Mach number, Reynolds number plane is shown on Fig. 8.

B. Application to Laser Absorption Problem

Applications of the modified algorithm to the laser absorption problem are given in Figs. 9-13. Figure 9 shows a representative grid with moderate stretching and a superimposed ray-traced laser beam. Representative convergence rates for the laser absorption calculation are shown in Fig. 10 for three cases: a direct method in which the laser rays and the fluid dynamics equations are solved directly and simultaneously; one with direct inversion of the fluids equations in which the laser ray

calculations are uncoupled; and one which uses the ADI method for the fluids equations and again is uncoupled from the laser beam. Clearly, the laser ray calculations should be coupled with the fluids equations, but the CPU requirements for the complete system remain quite large even though convergence is achieved in three to five iterations. Details of these techniques are to appear in Ref. 13.

Figure 11 shows temperature contours for laser absorption in argon at several laser power levels. These calculations are for a flow velocity of 1 cm/s, and ignore the effects of gravity. The effects of varying the inlet velocity at fixed laser power are seen to result in much greater movement of the heating zone as demonstrated in Fig. 12, while Fig. 13 demonstrates the effect of scaling up the laser size. This latter variation does not show strong movement of the plasma region, but size scaling beyond that indicated appears to result in conditions which no longer allow a steady solution. Present emphasis here is on improving the radiation loss model and investigating the effects of size scaling in more detail. The radiation loss model is described below.

C. Absorptivity Characteristics of Hydrogen Alkali Mixtures

To enable absorption predictions of solar energy, we are developing a broadband model of the absorption characteristics of hydrogen-alkali metal vapor mixtures. Alkali metal vapors are known to be efficient broadband absorbers of visible wavelengths. Theoretical studies have shown that the absorption of concentrated solar energy by alkali metal vapors is due to two mechanisms: photoionization and dimer transitions. The dimer absorption bands of metal vapors extend over most of the solar spectrum. For sodium and potassium, the strongest bands lie near the peak of the solar spectrum while for cesium these bands extend into the infra-red

region. When mixed with hydrogen, the alkali metal vapors will form hydrides that are also effective absorbers in the visible regime, but these additional absorption mechanisms are being ignored for now.

As an approximate representation of the absorption characteristics of alkali metals, we are attempting to model the radiative transfer in various wavenumber regimes as a series of bands. In each band, the molecular absorption coefficient is based upon the Franck Condon principle and uses a method called the quasi-static line-broadening principle. (From a classical viewpoint, the Franck Condon principle states that spontaneous transitions between electronic states are most likely to occur when the two nuclei are at their extreme vibrational positions. Further, it assumes that the accompanying photon absorption/emission takes place so rapidly that the positions of the nuclei do not change.) This quasi-static approximation requires the knowledge of the potential energy curves for the different molecular states and the oscillator strengths corresponding to each transition.

Under the quasi-static approximation, the probability of a transition occurring at frequency, ν , while the nuclei are separated by a distance, R , (here, $h\nu$ is the energy difference between the upper and lower states), can be used to estimate the molecular absorption coefficient:

$$k_{\nu}(\nu, T) = \frac{\pi^2 e^2}{2mc} f g [N]^2 R^2 \left| \frac{dR}{d\nu} \right| \exp \left[-\frac{V(R)}{KT} \right] \quad (2)$$

where f is the oscillator strength, g is the multiplicity of the lower electronic state, $V(R)$ is the binding energy, and other symbols have their standard meaning. The derivative $dR/d\nu$ in this expression is computed from

the potential energy diagrams of the molecule. Calculations based on Eqn. 2 for sodium shown good agreement with experimental spectra.

Although we are planning to use this approach as an interim, we are using an alternative procedure based upon a fit to existing experimental data,

$$k_v(v,T) = \frac{\pi^2 e^2}{2mc} fg N^2 G(v) \exp \left[-\frac{V(R)}{KT} \right] \quad (3)$$

where $G(v)$ is the line shape factor. For quasi-static broadening, this profile is Lorentzian,

$$G(v) = \frac{\gamma/\pi}{\Delta v^2 + \gamma^2} \quad (4)$$

Here, $\Delta v = v - v_0$ and γ is the linewidth parameter which is taken from experimental data. Representative absorption coefficients for sodium and potassium are given in Figs. 14 and 15 for various temperatures.

For the range of temperatures of interest (3000K to 5000K) broadband absorption of solar radiation by bound-free or photoionization transitions may also be important in the visible region. The semi-classical derivation for the bound-free absorption cross-section yields the Kramer's formula. Combining this with the Boltzman equation for the number of atoms in the n^{th} state, we obtain the bound-free absorption coefficient as,

$$k_v^{-1} = \frac{64 \pi^4}{3\sqrt{3}} \frac{e^{10} m Z^4 N}{h_6 c v^3} \sum_n \frac{1}{n^3} e^{-(E_1 - E_n)/KT} \quad (5)$$

where E_1 is the energy of the electron in the ground state and E_n is the energy of the n^{th} state. Figure 16 shows the bound-free absorption

coefficient of Na at a temperature of 5000K. The total absorption coefficient of an alkali metal vapor is the sum of the dimer and bound-free coefficients.

D. Radiation Loss Modeling

Once the absorptivity characteristics of the working fluid are determined, the next step is to develop a model for predicting the radiative losses from the hot zone. Because the radiative flux that appears in the energy equation arises because of a volumetric, rather than a local, effect its evaluation requires inordinately large amounts of computer time and, consequently, it must be modeled rather than computed. This volumetric dependence also means that no simple scaling laws can be developed for the general case.

The engineering model we are using to compute the radiative flux in the energy equation is divided into two separate contributions. First, the direct absorption of the solar energy by the hydrogen/seedant mixture is computed directly by solving the radiative transfer equation along discrete rays of concentrated solar beam. The only approximation here is a subdivision of the broad-band radiation into distinct bands.

The second contribution to the radiation flux term is the re-radiation by the hot gases and the confining walls. The radiation from the hot gases is being modeled by a differential approximation to the complete equation of transfer, the so-called P1 approximation. The P1 equation at a particular frequency is given by,

$$\frac{\partial}{\partial x} \frac{\gamma}{k_v} \frac{\partial G_v}{\partial x} + \frac{\partial}{\partial y} \frac{\gamma}{k_v} \frac{\partial G_v}{\partial y} = 3k_v \gamma (G_v - 4\pi I_0 v) \quad (6)$$

where G_v is the incident radiation. The source term in the energy equation is then computed from G_v by,

$$\nabla \cdot q_v^Y = k_v (4\pi I_{bv} - G_v) \quad (7)$$

The representation of the frequency dependence requires a further approximation. Standard methods for incorporating wavelength variations include the Planck and Rosseland mean free paths. These averages have the advantage of retaining the simplicity of the grey formulations, but neglect important contributions from optical windows. The alternative is to employ a simple box model for the various bands in the system. Here, we are using a band model along with the P1 differential approximation.

The spectral information from the detailed description of the absorptivity given above is used to identify the appropriate bands and an average absorption coefficient is used in each band. Preliminary solar energy absorption calculations in a flowing gas based upon a four-band model are given in Figs. 17 to 19. The use of a four-band model implies four P1 equations must also be coupled with the solar energy absorption and the energy equation. (For these initial results, the flowfield was assumed to be one-dimensional and uniform, $p_v=0$, $p_u=\text{constant}$, and the absorptivity variation with temperature was ignored.) Figure 17 shows heat addition contours for an energy size of 125N. Figures 18 and 19 show temperature contours for two wall temperature cases. Coupling with the low Mach number equations described above is currently being initiated along with temperature-dependent absorptivity.

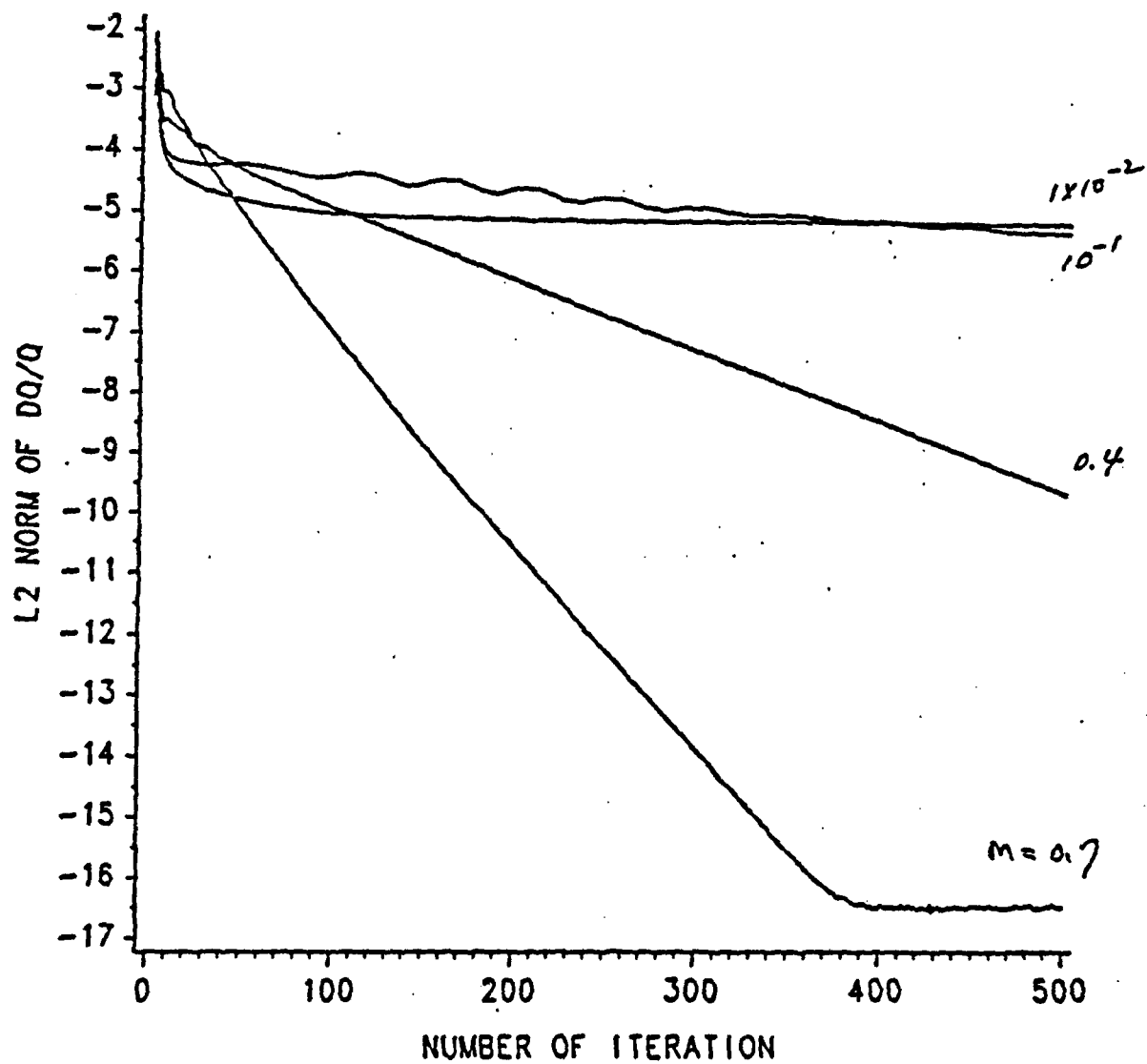


Fig. 1. Convergence of transonic time dependent algorithms at various Mach number conditions for a two-dimensional flowfield.

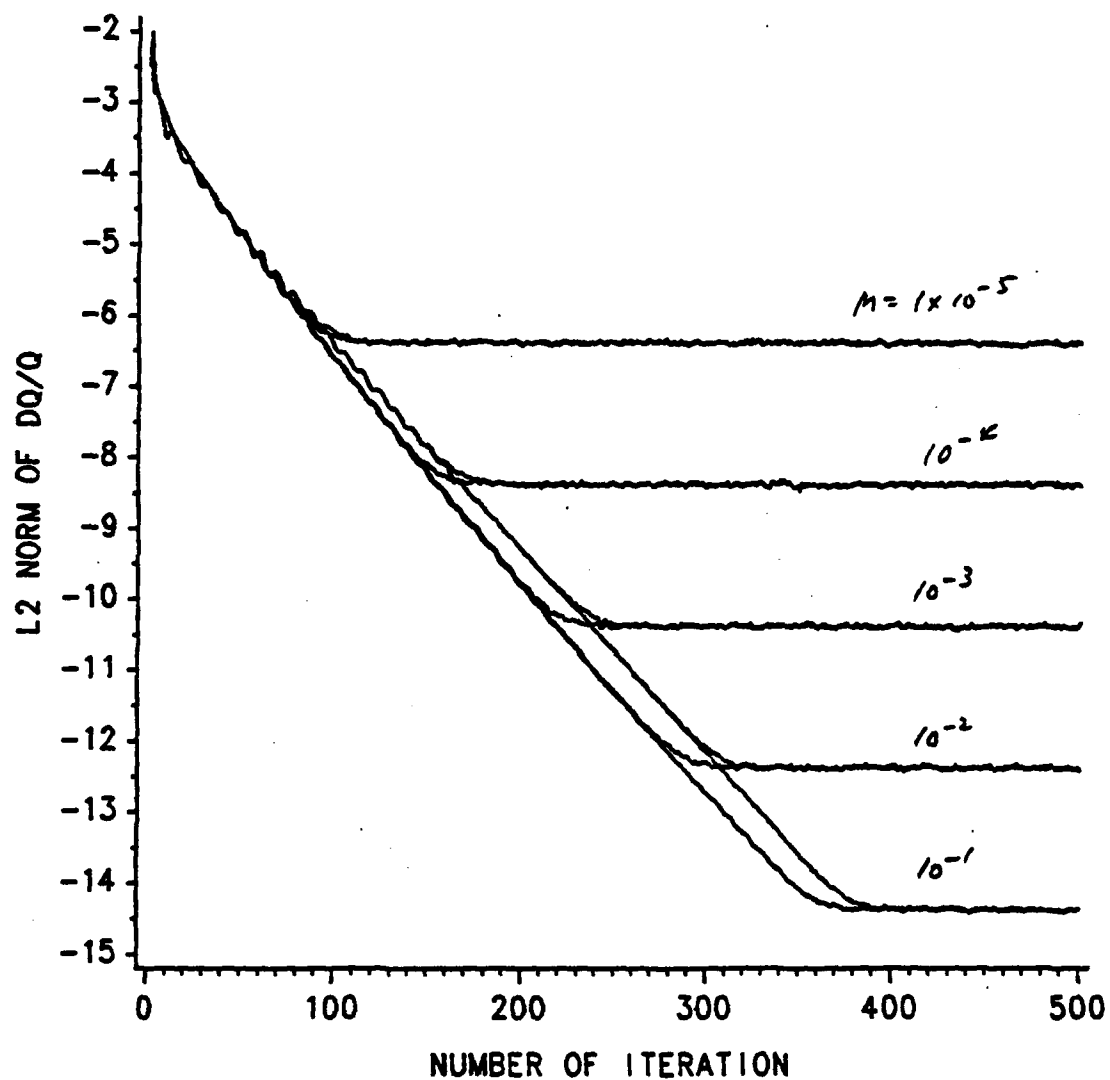


Fig 2. Convergence of Euler Implicit scheme for the two dimensional compressible Euler equations using preconditioning for various Mach numbers, CFL=5, $\omega_g=0.25$. Convergence plot shown is for the continuity and x-momentum equation.

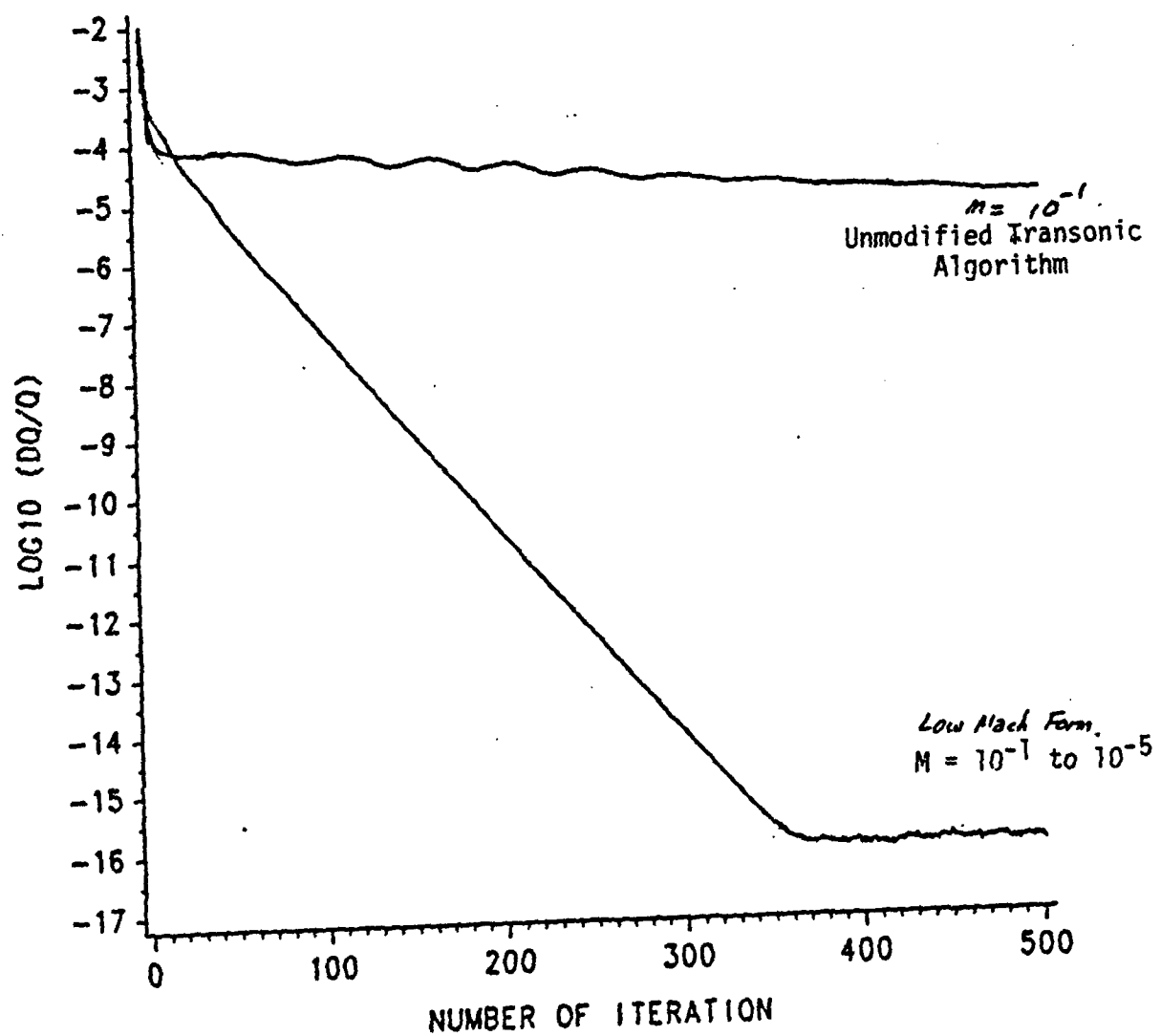


Fig. 3. Convergence rate of low Mach number time dependent algorithm for Mach number conditions down to 10^{-5} . For comparison, the convergence rate of the original algorithm is shown at a Mach number of 0.10.

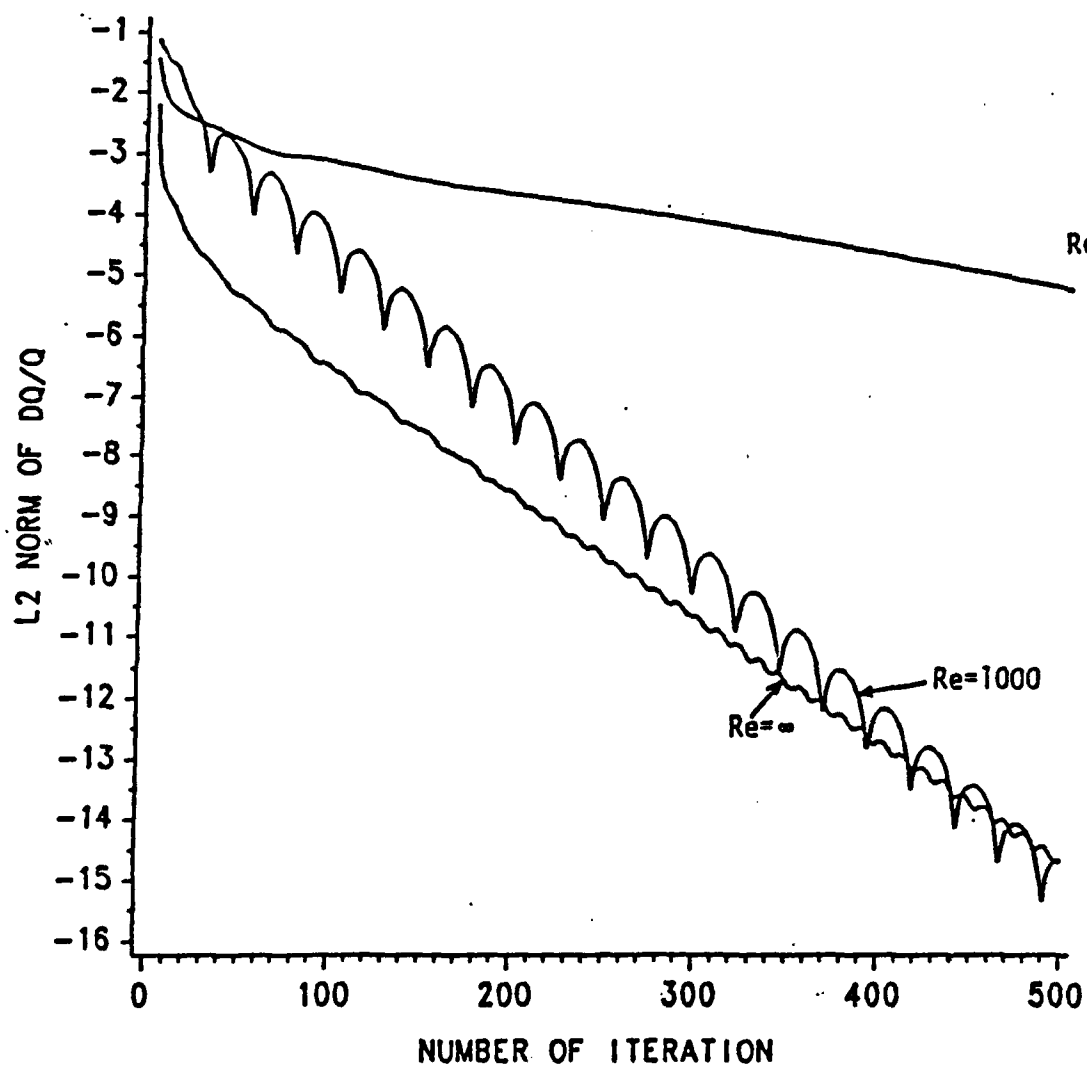


Fig. 4. Convergence rates of low Mach number viscous formulation for various Reynolds numbers. Present results are for a flow Mach number of 10^{-4} .

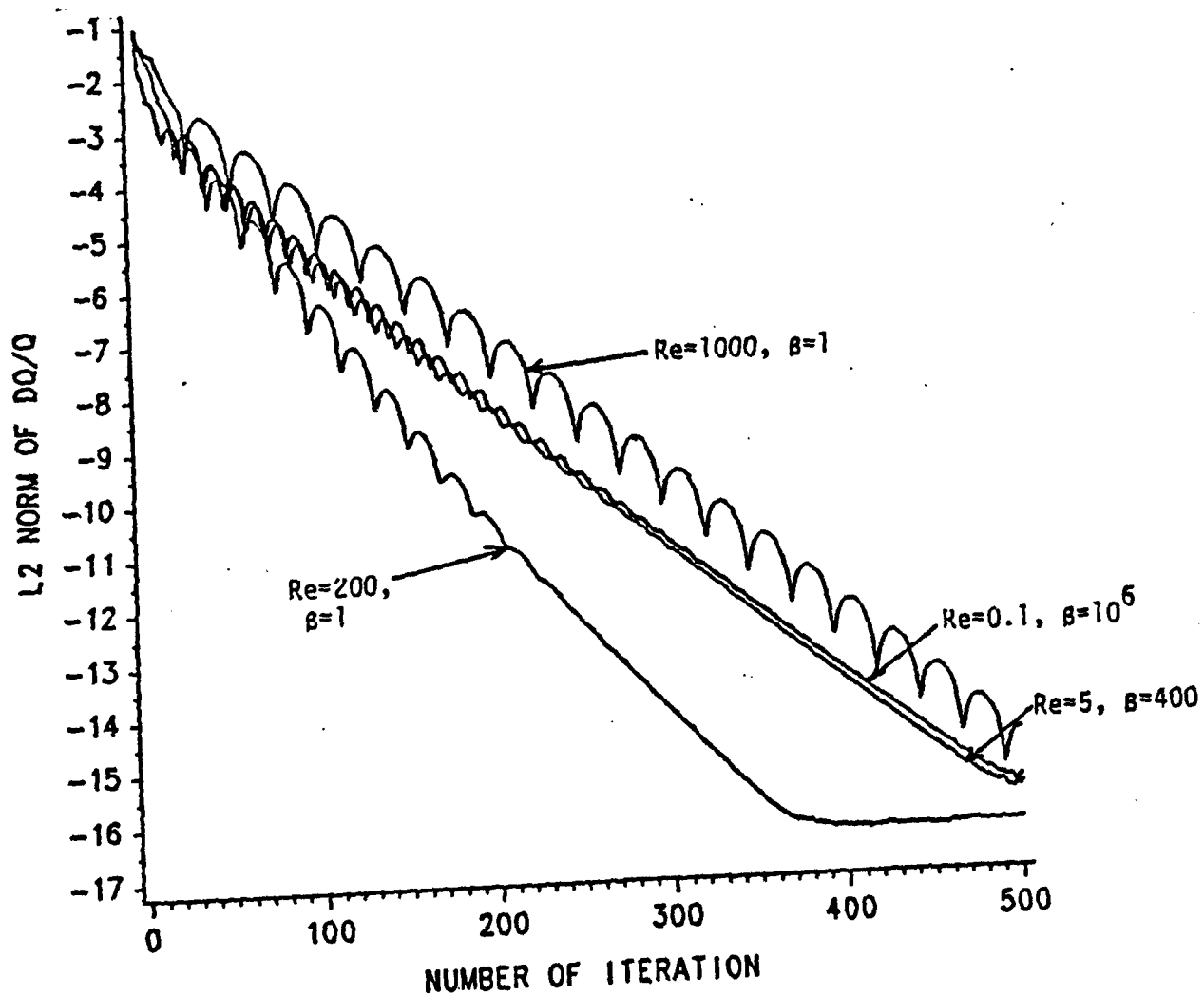
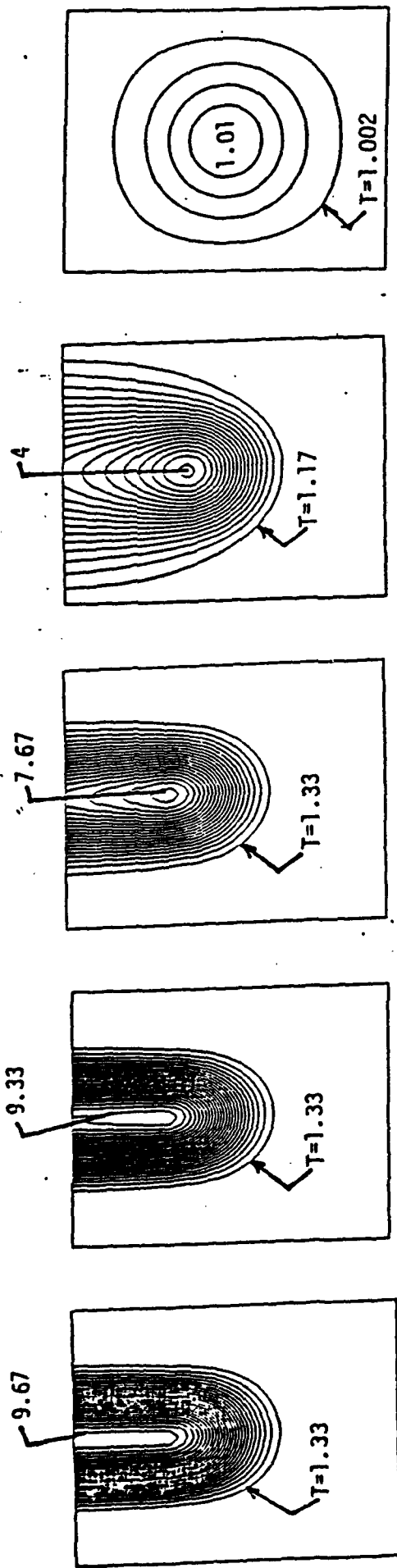
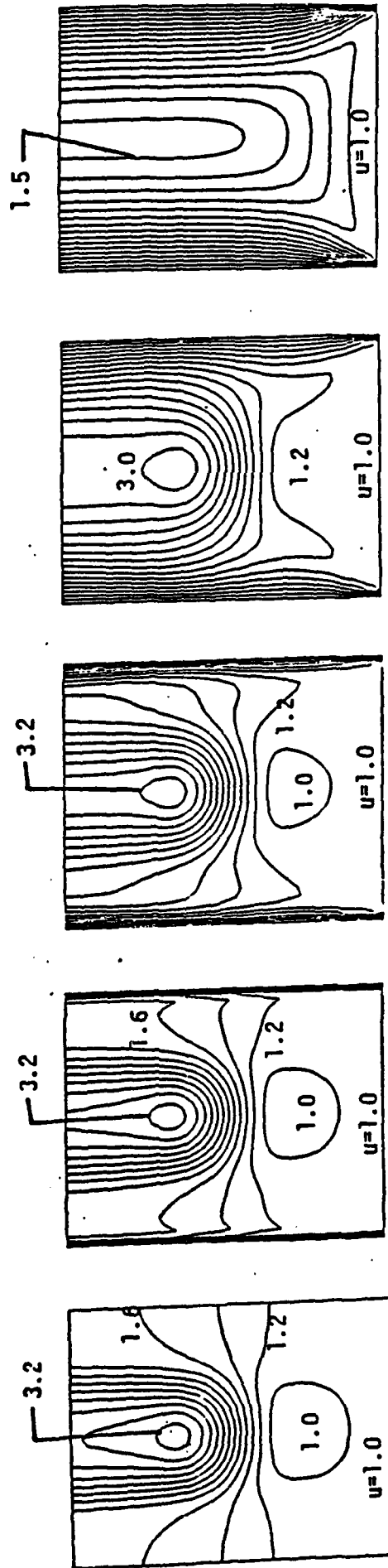


Fig. 5. Convergence rates of low Mach number viscous formulation using optimum values of time-stepping parameter, β .



(a) Temperature Contours



(b) Velocity Contours

$Re=\infty, \beta=1$

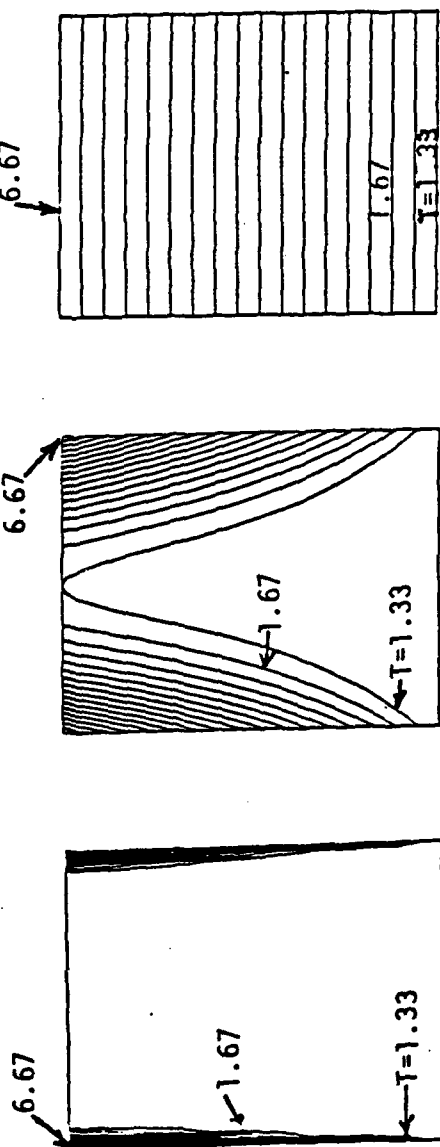
$Re=5000, \beta=1$

$Re=500, \beta=1$

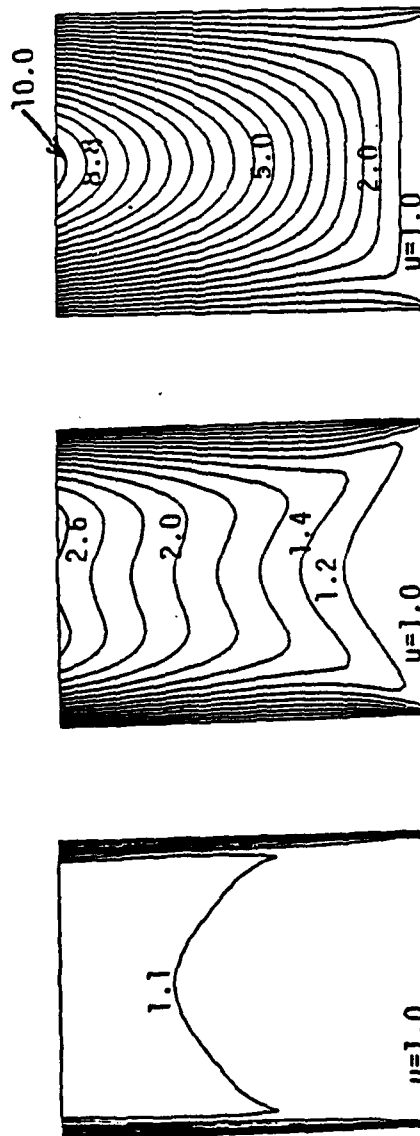
$Re=50, \beta=4$

$Re=0.05, \beta=4 \times 10^6$

Fig. 6. Flowfield solutions for specified heat addition in a duct at various Reynolds numbers. All calculations at a Mach number of 0.5×10^{-3} .



(a) Temperature



(b) Velocity

$Re=5000, \beta=1$

$Re=50, \beta=4$

$Re=0.05, \beta=4 \times 10^6$

Fig. 7. Flowfield solutions for flows with strong wall heat transfer over a wide range of Reynolds numbers. Flow Mach number, 0.5×10^{-3} .

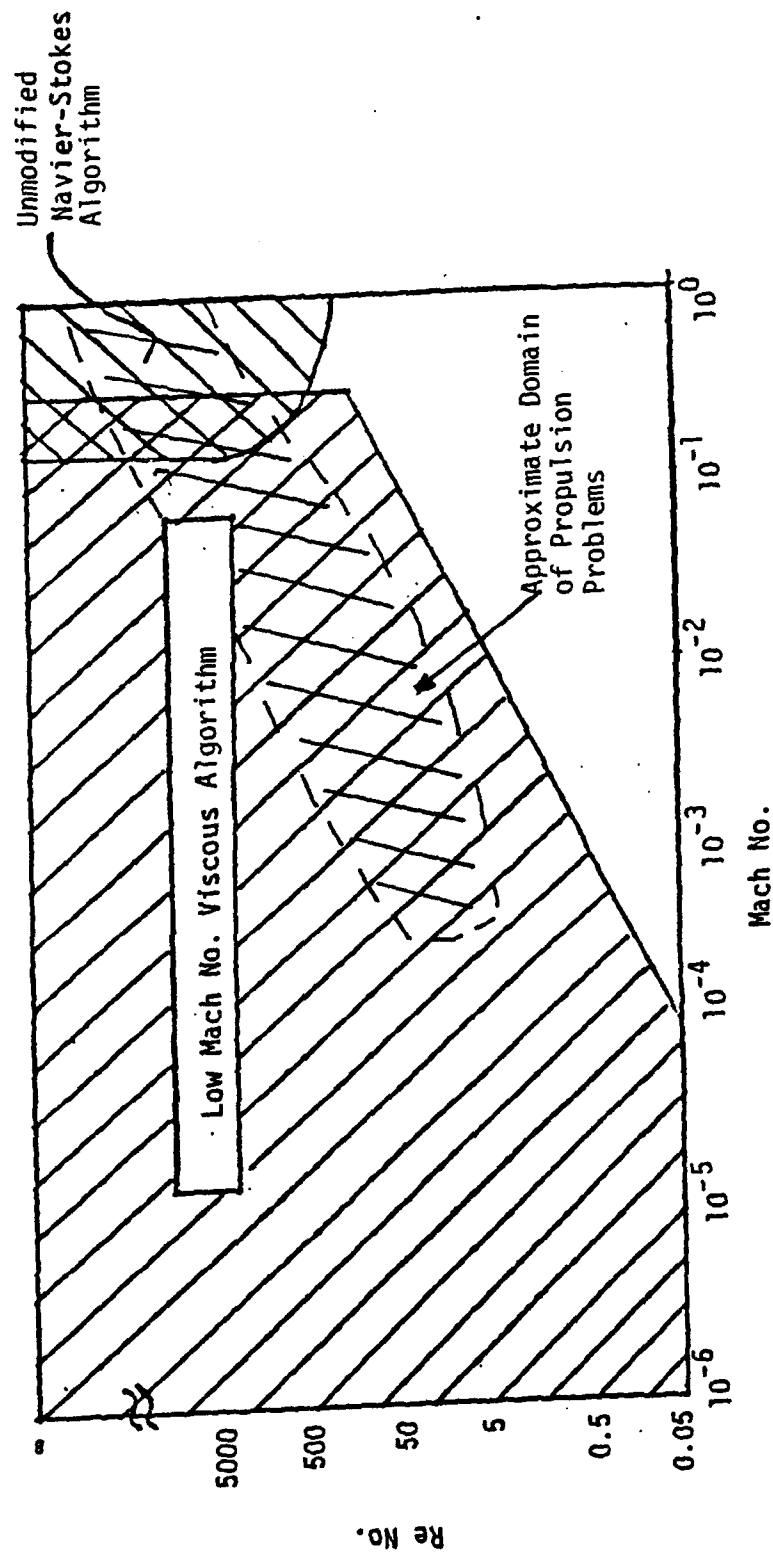


Fig. 8. Mach number-Reynolds number convergence regime for regional time dependent algorithm and for modified low Mach number viscous formulation showing approximate regime of energy addition problems in propulsion.

Absorption Chamber Geometry
(51 x 31 Grid)

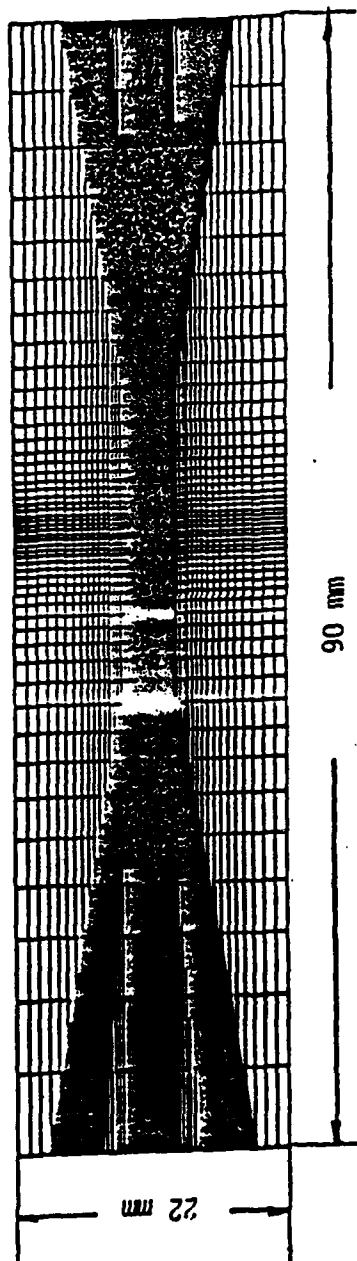


Fig. 9. Absorption chamber geometry showing stretched fluid dynamics grid (51 x 31) and laser ray comprising a doughnut-shaped beam.

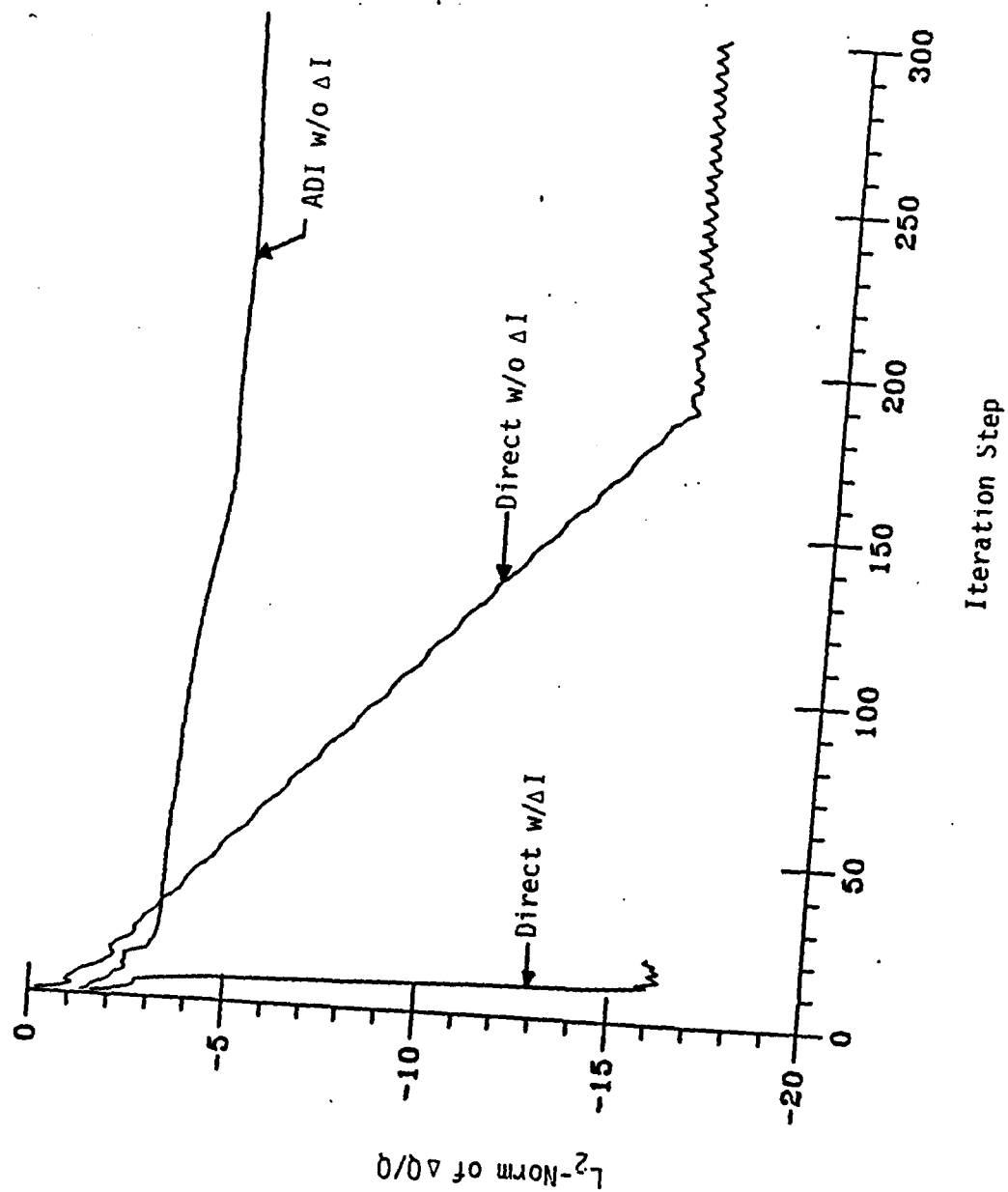


Fig. 10. Convergence rates for laser absorption problem for various time dependent methods.

Temperature Field with Laser Power Variation

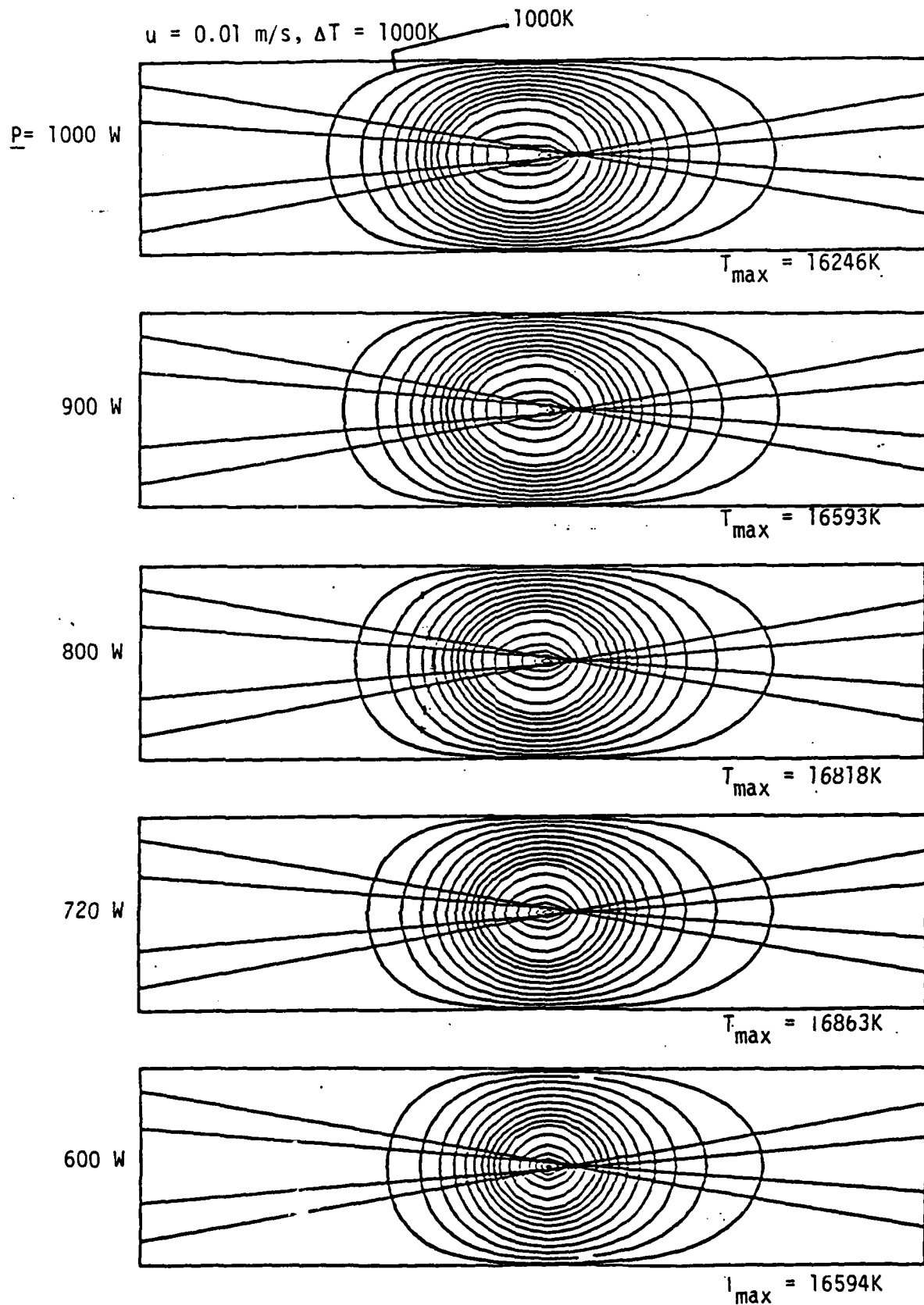


Fig. 11. Representative temperature contours for laser absorption in argon as a function of laser power.

Temperature Field with Velocity Variation

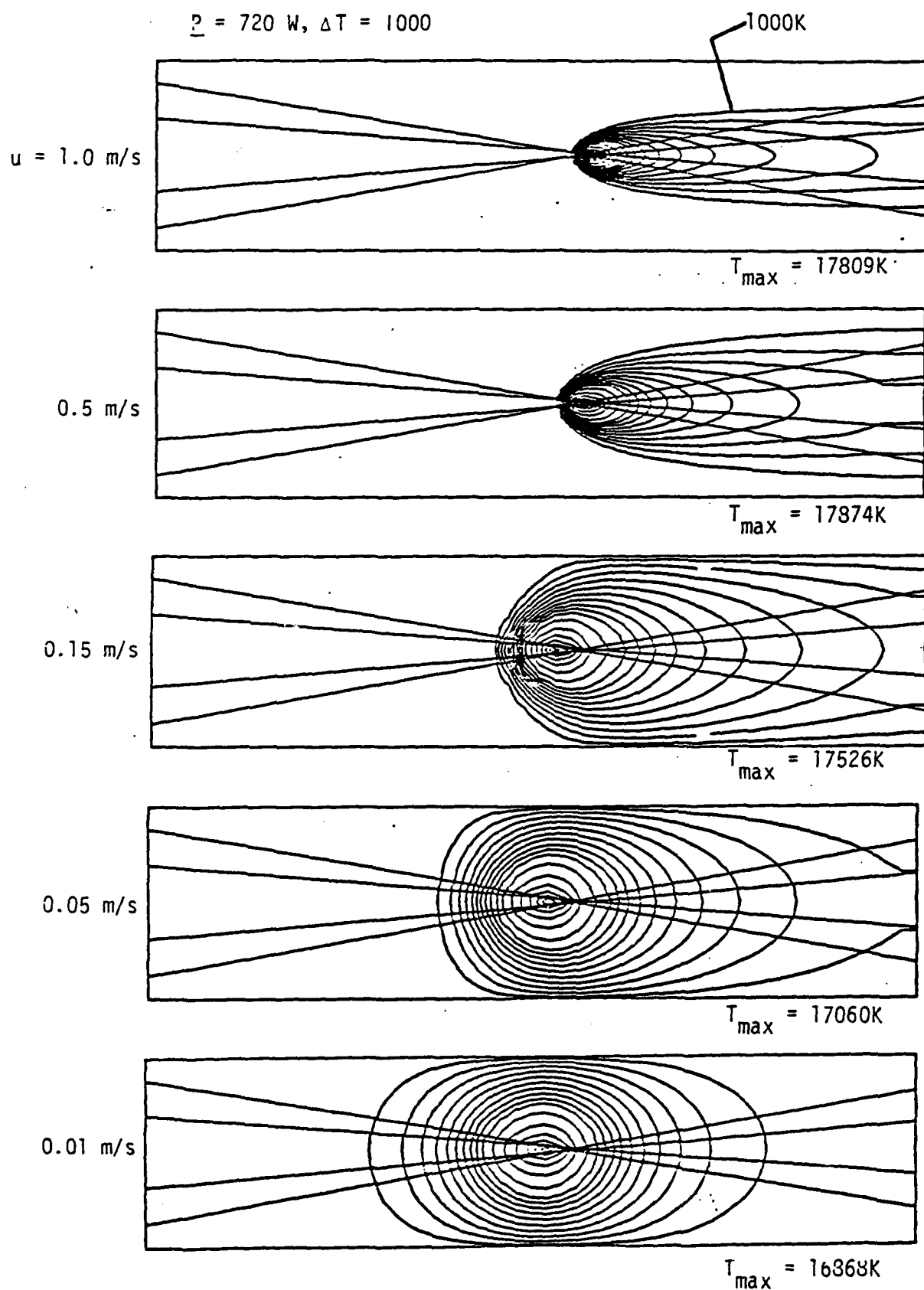


Fig. 12. Temperature contours in laser absorption regime. Fixed laser power and varying inlet velocity.

Temperature Field with Chamber Geometry Variation

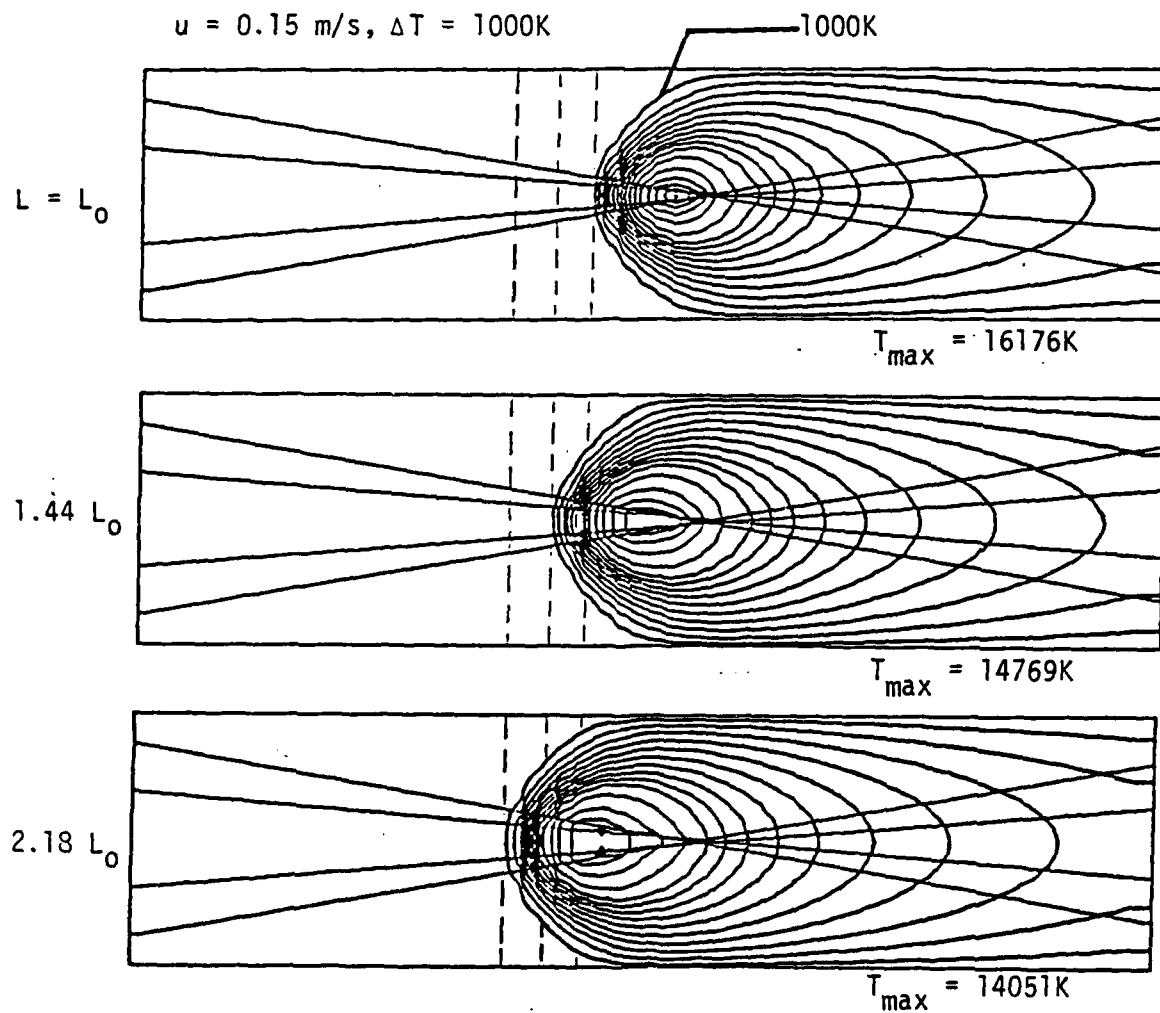


Fig. 13. Effects of scaling laser power.

DIMER ABSORPTION Na_2 TEMP=500,2500,5000

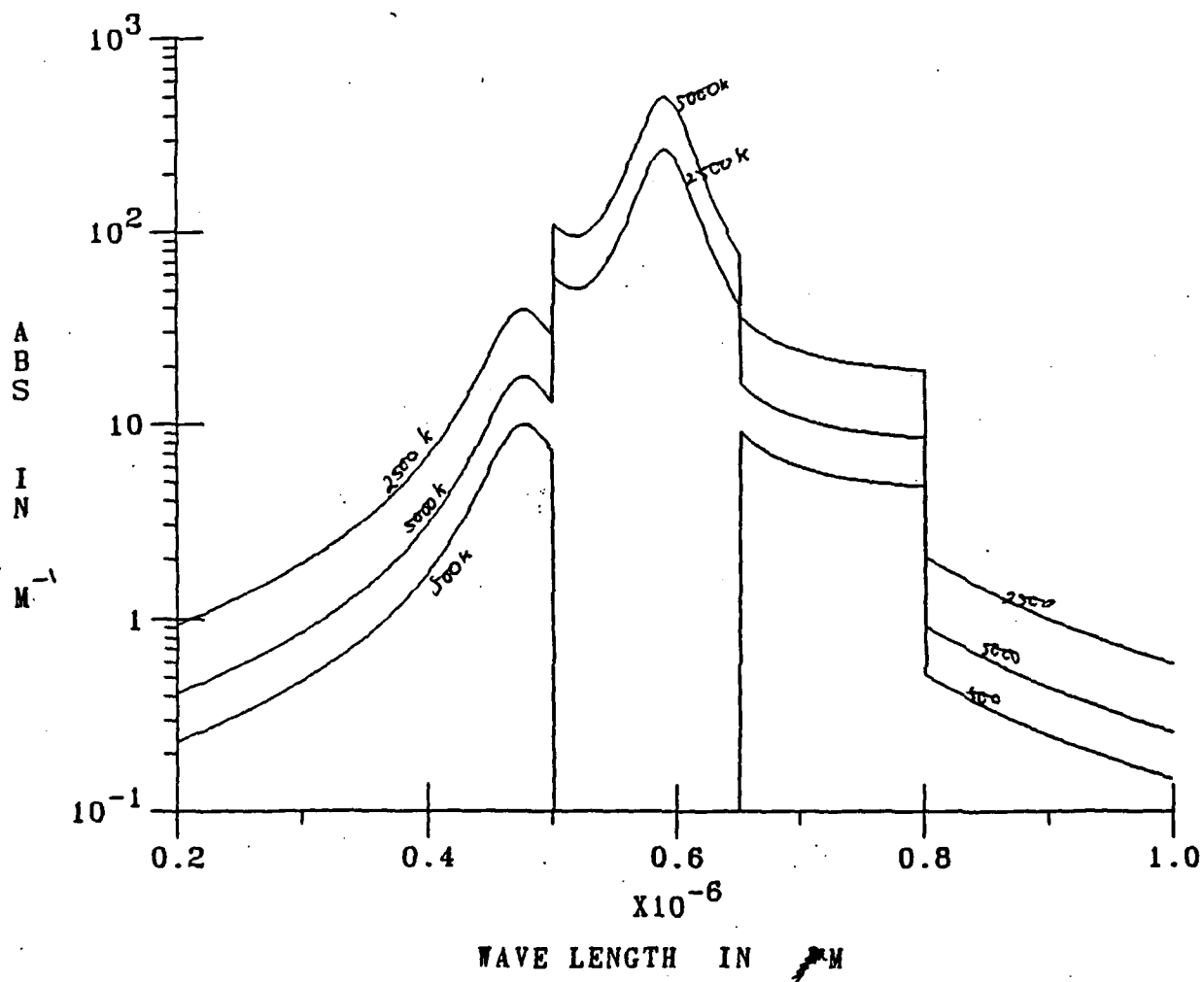


Fig. 14. Dimer absorption characteristics of sodium at 500, 2500, and 5000K based on four-band model.

DIMER ABSORPTION OF K_2 TEMP=2000,4000K

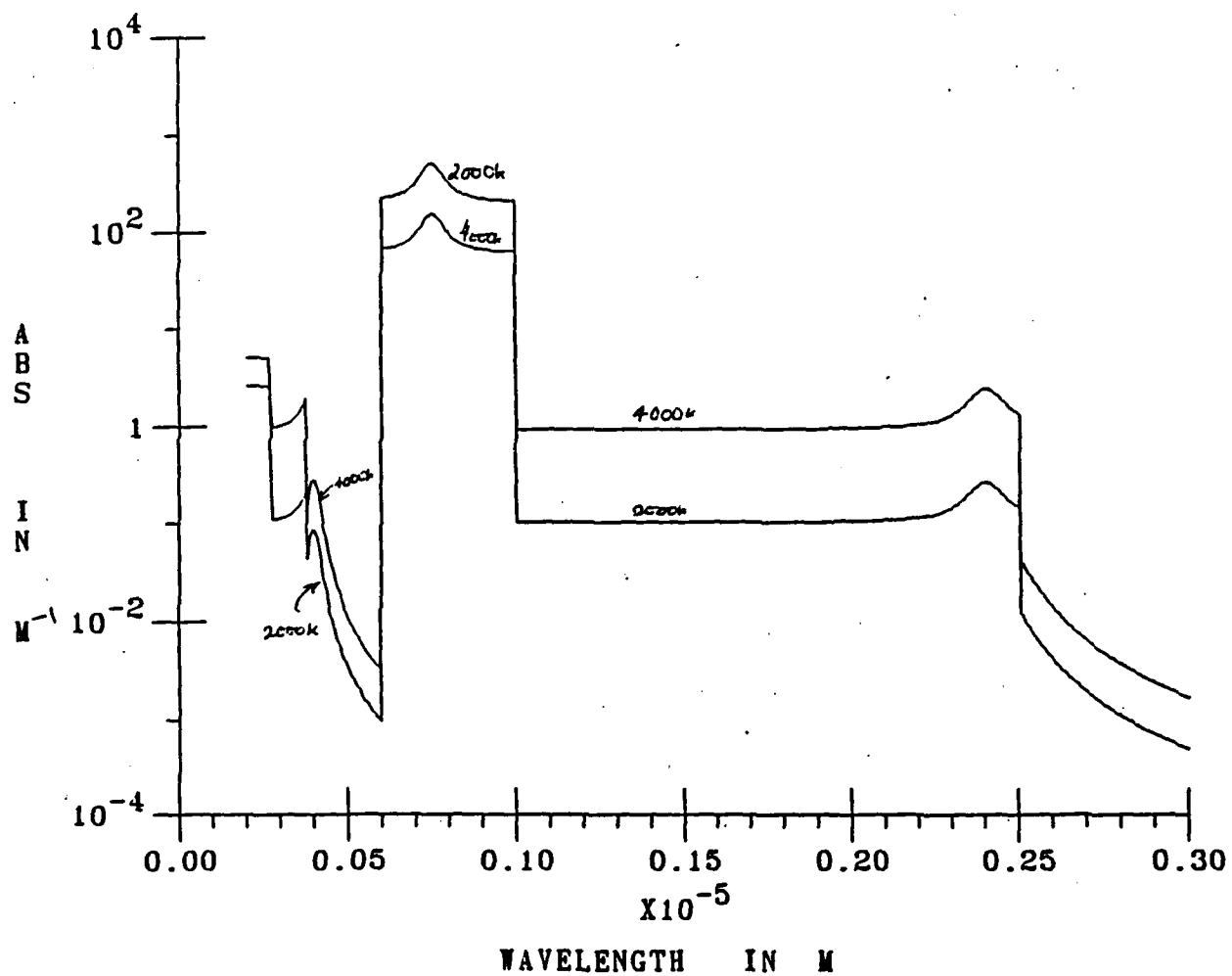


Fig. 15. Dimer absorption characteristics of potassium at 2000 and 4000K based on band model.

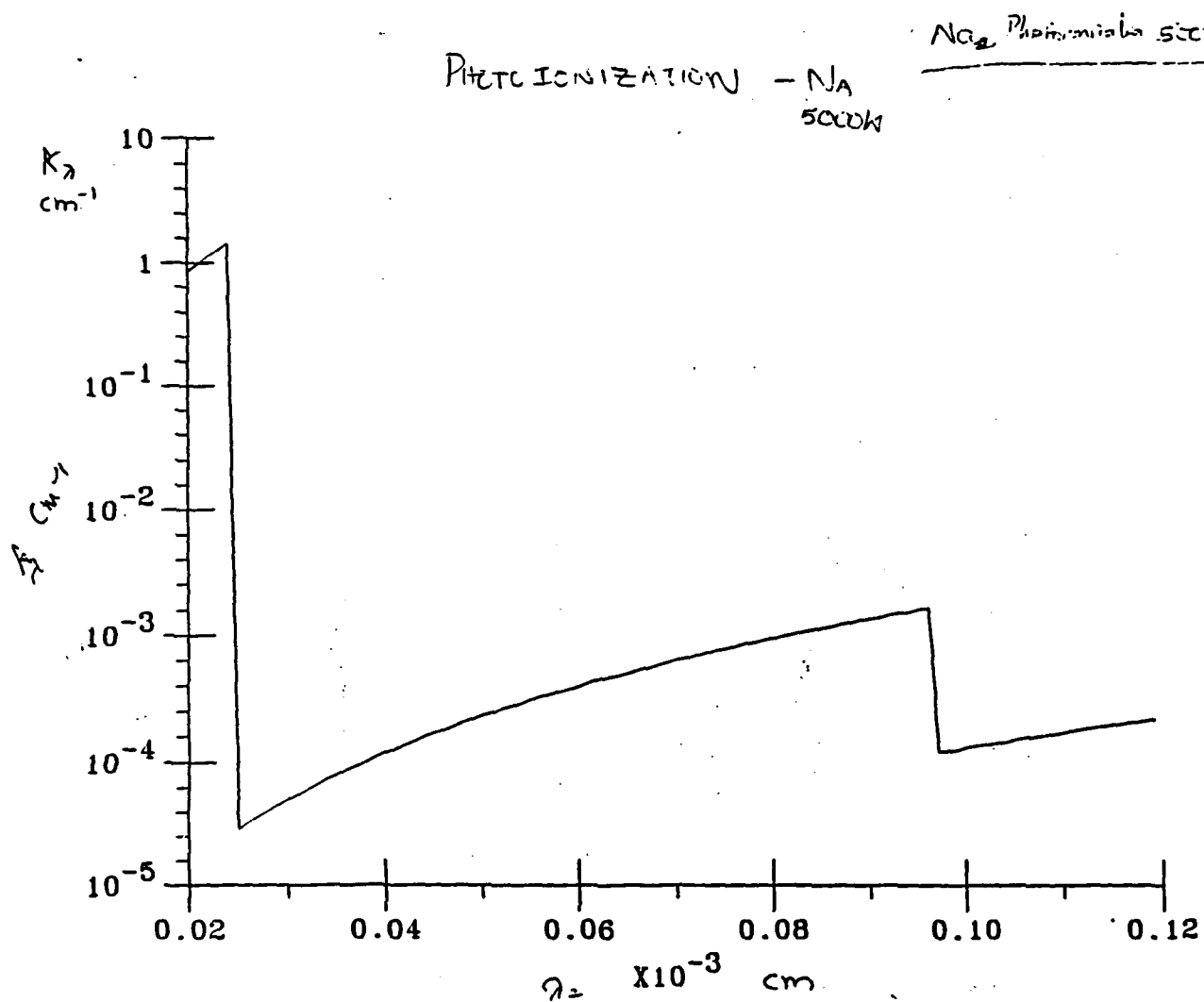


Fig. 16. Photoionization absorption coefficient of sodium at 5000K.

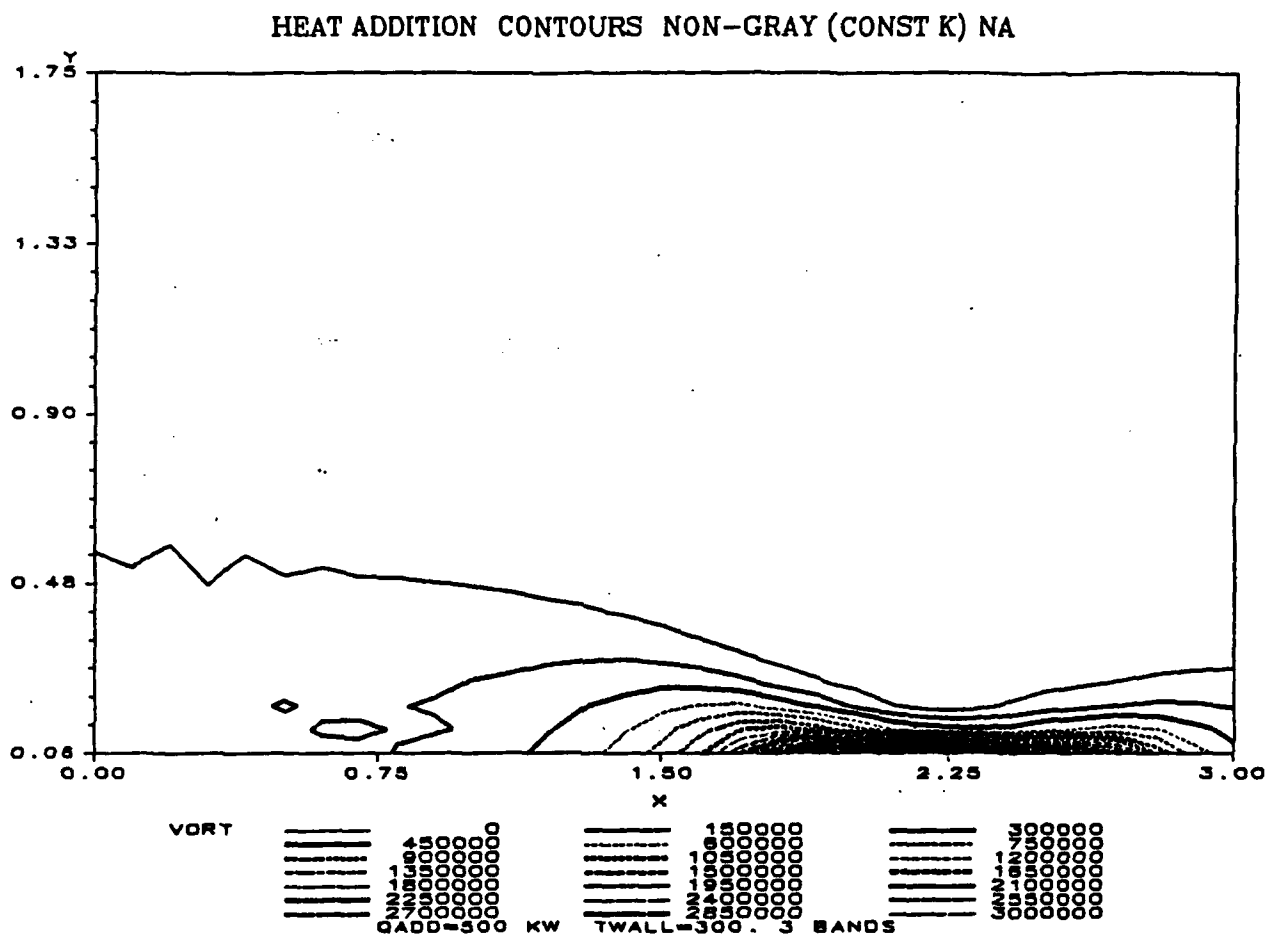


Fig. 17. Heat addition contours for non-gray (constant k) sodium.

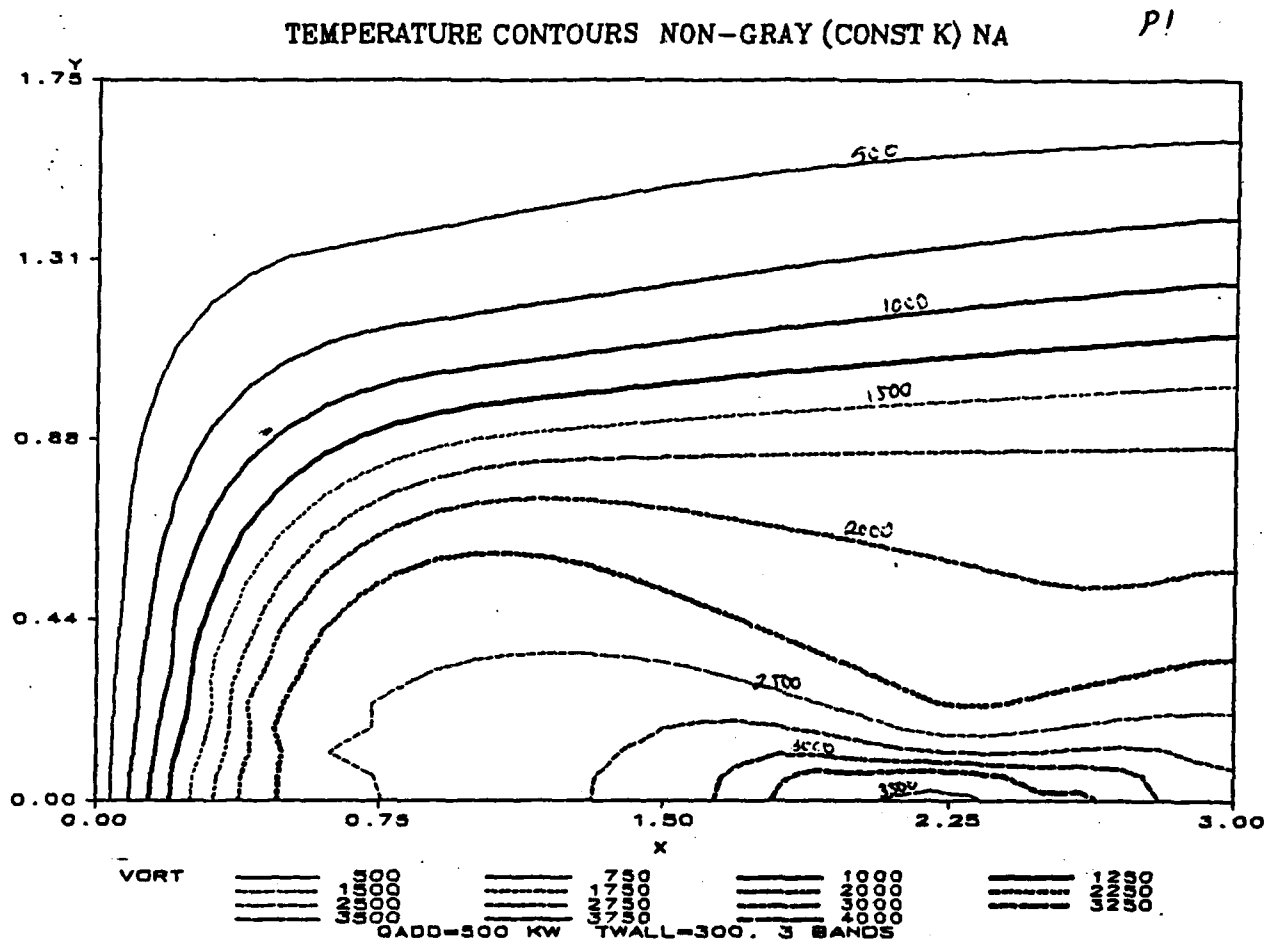


Fig. 18. Temperature contours for non-gray sodium with absorptivity independent of temperature. $T_w = 300K$.

II. A CUMULATIVE CHRONOLOGICAL LIST OF WRITTEN PUBLICATIONS

1. Merkle, C. L. and Gulati, A., "The Absorption of Electromagnetic Radiation in an Advanced Propulsion System", J. Spacecrafts and Rockets, Vol. 21, No. 1, Jan.-Feb. 1984, pp. 101-107.
2. Merkle, C. L., "The Potential for Using Laser Radiation to Supply Energy for Propulsion", Orbit Raising and Maneuvering Propulsion: Research Status and Needs, AIAA Progress in Astronautics and Aeronautics Series, L. H. Caveny, Ed., AIAA, New York, 1984, pp. 48-72.
3. Merkle, C. L., "The Use of Electromagnetic Radiation as an Energy Source for Propulsion", Proceedings of Workshop on Advanced Propulsion Concepts Using Time Varying Electromagnetic Fields, Michigan State University Press, 1984.
4. Merkle, C. L., "Prediction of the Flowfield in Laser Propulsion Devices", AIAA Paper 83-1445, AIAA 18th Thermophysics Conference, Montreal, Canada, May 1983. AIAA Journal, Vol. 22, No. 8, Aug. 1984, pp. 1101-1107.
5. Merkle, C. L., Gulati, A., Choi, Y.-H., "The Effect of Strong Heat Addition on the Convergence of Implicit Schemes", AIAA Paper 83-1914, AIAA 6th Computational Fluid Dynamics Conference Proceedings, Danvers, MA, July 1983, pp. 212-221. AIAA Journal, Vol. 23, No. 6, June 1985, pp. 847-855.
6. Merkle, C. L., Molvik, G. A. and Choi, D., "A Two-Dimensional Analysis of Laser Heat Addition in Converging Nozzles", AIAA Journal, Vol. 23, No. 7, July 1985, pp. 1053-1060.
7. Merkle, C. L., "Stability of Absorption Phenomena in Laser-Thermal Propulsion Gasdynamic Interaction", AIAA Paper 84-1571, AIAA 17th Fluid Dynamics, Plasmadynamics & Lasers Conference, Snowmass, CO, June 1984.
8. Merkle, C. L., Molvik, G. A. and Shaw, Eric J.-H., "Numerical Solution of Strong Radiation Gasdynamic Interactions in a Hydrogen-Seedant Mixture", J. Propulsion and Power, Vol. 2, No. 5, September-October 1986, pp. 465-473.
9. Merkle, C. L. and Choi, Y.-H., "Computation of Low-Speed Flow with Heat Addition", AIAA Journal, Vol. 25, No. 6, June 1987, pp. 831-838.
10. Merkle, C. L. and Choi, Y.-H., "Computation of Low Mach Number Flows With Buoyancy", Proceedings of the 10th International Conference on Numerical Methods in Fluid Dynamics, Beijing, China, June 23-27, 1986, pp. 169-173.
11. Merkle, C. L. and Hosangadi, A., "Computation of Low Speed Viscous Flows with Heat Addition", Sixth IMACS International Symposium on Computer Methods for Partial Differential Equations, Lehigh University, June 23-26, 1987, Bethlehem, PA.

12. Merkle, C. L. and Choi, Y.-H., "Computation of Low-Speed Compressible Flows with Time-Marching Procedures", to appear in the International Journal for Numerical Methods in Engineering.
13. Merkle, C. L., "Numerical Solution of Flowfields with Strong Radiation", submitted for presentation at the ASME Winter Annual Meeting, Symposium on Advances and Applications in Computational Fluid Mechanics in Chicago, IL, November 28-December 2, 1988.
14. Thynell, S. T. and Merkle, C. L., "Two-Dimensional Analysis of Solar Absorption in a Gas", submitted to Journal of Solar Engineering.

III. PROFESSIONAL PERSONNEL ASSOCIATED WITH RESEARCH EFFORT

Professional Staff -

Charles L. Merkle, Principal Investigator, Professor, Mechanical Engineering

Graduate Students -

Michael J. Stanek, Graduate Assistant, February 1981-August 1982. M.S. Thesis title, "Analytical Studies of the Absorption Mechanisms of Equilibrium Hydrogen." Present position: Captain, US Air Force, AFWAL/POTC, WPAFB, OH.

Anil Gulati, Graduate Assistant, September 1981-August 1983. M.S. Thesis title, "The Absorption of Electromagnetic Radiation in an Advanced Propulsion System." Present position: Research Scientist, GE Corporate Research and Development Center, Schenectady, NY.

Gregory A. Molvik, Graduate Assistant, September 1982-January 1985. M.S. Thesis title, "A Two-Dimensional Analysis of Laser Heat Addition in Converging Nozzles". Permanent address: CFD Group, NASA/Ames, Moffett Field, CA. Presently on leave as Ph.D. student at Penn State.

Peter Tsai, Graduate Assistant, September 1983-August 1985. M.S. Thesis title, "Stability Characteristics of Laser-Supported Plasmas". Present position: Ph.D. Candidate Penn State University.

Yun-Ho Choi, Ph.D. Candidate, January 1985 to present. Ph.D. Thesis title, "Computation of Low Mach Number Flowfields with Strong Heat Addition".

Eric Shaw, Graduate Assistant, September 1984 to May 1986. M.S. Thesis title, "Laser Absorption in Flowing Gas". Present position, Ph.D. Candidate, Pennsylvania State University.

Ashvin Hosangadi, Ph.D. Candidate, September 1985-present.

Sankaran Venkateswaran, Ph.D. Candidate, September 1985-present, "Absorption of Solar Energy in Hydrogen Alkali Metal Vapor Mixtures".

IV. INTERACTIONS/SPOKEN PRESENTATIONS

"Analysis of Laser-Supported Combustion Waves in Flowing Media", AFOSR/AFRPL Rocket Propulsion Research Meeting, Lancaster, CA, March 26, 1981.

"The Potential for Using Laser Radiation as an Energy Source for Propulsion", Orbit Raising Propulsion Workshop, Orlando, FL, January 16, 1982.

"The Use of Electromagnetic Radiation as an Energy Source for Propulsion", Symposium on Advanced Propulsion Concepts Using Time-Varying Electromagnetic Fields, East Lansing, MI, February 4, 1982.

"Analysis of Laser-Supported Plasmas in Flowing Media", AFOSR/AFRPL Rocket Propulsion Research Meeting, Lancaster, CA, March 3, 1982.

"The Absorption of Electromagnetic Radiation in an Advanced Propulsion System", AIAA Electric Propulsion Meeting, New Orleans, LA, November 19, 1982.

"Prediction of the Flowfield in Laser Propulsion Devices", AIAA 18th Thermophysics Conference, Montreal, Canada, May 1983.

"The Effect of Strong Heat Addition on the Convergence of Implicit Schemes", AIAA 6th CFD Conference, Danvers, MA, June 1983.

"A Two-Dimensional Analysis of Laser Heat Addition in Converging Nozzles", AIAA Aerospace Sciences Meeting, Reno, NV, January 1984.

"High Power Nd-Glass Laser Instrument for Advanced Propulsion and Diagnostics", AFOSR/AFRPL Rocket Propulsion Research Meeting, Lancaster, CA, March 12-15, 1984.

"Stability of Absorption Phenomena in Laser-Thermal Propulsion Gasdynamic Interaction", AIAA 17th Fluid Dynamics, Plasmadynamics & Lasers Conference, Snowmass, CO, June 25-27, 1984.

"Analytical Modeling of Strong Radiation Gasdynamic Interaction", AFOSR/AFRPL Chemical Rocket Research Meeting, Lancaster, CA, March 20, 1985.

"Numerical Solution of Strong Radiation Gasdynamic Interactions", AIAA 18th Fluid Dynamics, Plasmadynamics & Lasers Meeting, Cincinnati, OH, July 16-18, 1985.

"An Implicit Time-Dependent Scheme for Low Speed Flow with Buoyancy", 22nd Annual Meeting Society of Engineering Science, Inc., University Park, PA, Oct. 7-9, 1985.

"Computation of Compressible Flows at Very Low Mach Numbers", AIAA Aerospace Sciences Meeting, Reno, NV, Jan. 6-9, 1986.

"Computation of Low Mach Number Flows With Buoyancy", presented at the 10th International Conference on Numerical Methods in Fluid Dynamics, Beijing, China, June 23-27, 1986.

"Numerical Solution of Strong Radiation Gas Dynamic Interactions", AFOSR/AFRPL Chemical Rocket Research Meeting, Lancaster, CA, September 1986.

"Computation of Low Speed Viscous Flows with Heat Addition", presented at the Sixth IMACS International Symposium on Computer Methods for Partial Differential Equations, Lehigh University, June 23-26, 1987, Bethlehem, PA.

"Coupling Between Concentrated Solar Radiation and Gasdynamics", AFOSR/AFRPL Chemical Rocket Research Meeting, State College, PA, June, 1987.

V. INTERACTIONS/ADVISORY FUNCTIONS

Member of Workshop Panel, "Concepts and Experiments", NASA/Michigan State Symposium on Advanced Propulsion Concepts Using Time-Varying Electromagnetic Fields, February 1982.

"Aerospace Propulsion at Penn State", presentation to General Robert T. Marsh, USAF, The Pennsylvania State University, University Park, PA, May 5, 1982.

"Modeling of Flowfields that Interact with Radiation Fields", AFRPL/UDRI Solar Plasma Propulsion Workshop, Bergamo Center, Dayton, OH, Jan. 21-22, 1986.

VI. NEW DISCOVERIES

See Publication List.

END

DATED

FILM

8-88
STIC